Biodegradation of Atrazine by Atrazine Chlorohydrolase: Characterization of Mutant Enzyme and Immobilization System for Water Purification.

A THESIS SUBMITTED TO THE FACULTY OF THE GRADUATE SCHOOL OF THE UNIVERSITY OF MINNESOTA BY

Amit Aggarwal

IN PARTIAL FULFILLMENT OF THE REQUIREMENTS FOR THE DEGREE OF MASTER OF SCIENCE

Lawrence P. Wackett & Ping Wang

JANUARY 2012

Acknowledgement

I want to thank my advisor, Dr. Larry Wackett, for the opportunity to work in his laboratory, his support and patience, and for allowing me to work independently and always being there to guide me.

I would like to thank my mentor Dr. Jennifer Seffernick, for training me on different techniques in laboratory, and patiently helping me out throughout my association with the lab and teaching me good laboratory practices for research. Thank you so much for taking me under your wing. You are the best mentor I ever had.

I would also like to thank Dr. Alptekin Aksan and Dr. Mike Sadowsky for guiding us throughout the immobilization of atrazine chlorohydrolase project. Dr. Alptekin Aksan guided us in development of a robust and efficient immobilization system and Dr. Mike Sadowsky provided us with valuable direction about making the immobilization system safe to be used in water purifications systems.

I would like to thank my administrative adviser Dr. Ping Wang for always being supportive of my work and helping me out with planning my degree and ensuring that I meet all requirements in time. I am thankful to each of my committee members, Dr. Larry Wackett, Dr. Ping Wang and Dr. Jonathan Schilling for their time, for reading my thesis and for all the helpful suggestions.

Thanks goes to Erik Reynolds, Eduardo Reatgui and Lisa Kasinkas for being a great team on the immobilization project and making the work meticulously planned and fun; and other current and past Wackett lab members Janice Frias, Dave Sukovich, Neissa Pinzon, Kelly Aukema, Tony Dodge, Adam Erickson, Jasmine Erickson, Deep Golwala, Jack Richman and Michael Turnbull.

This research was supported by an NSF grant (CBET-0644784) to Dr. Alptekin Aksan, a research grant from Syngenta to Dr. Larry Wackett, Dr. Alptekin Aksan and Dr. Mike Sadowsky; and a seed grant to Dr. Larry Wackett and Dr. Alptekin Aksan from the Biotechnology Institute at University of Minnesota.

Dedication

I would like to dedicate this dissertation to my family and friends for their unwavering support throughout this process.

Abstract

Atrazine is the most widely used herbicide by corn and sorghum growers. Atrazine chlorohydrolase (AtzA) dechlorinates atrazine, producing non-toxic and non-phytotoxic hydroxyatrazine. In this study, we report the cloning and initial experiments for partial characterization of mutant AtzA (Colin Scott, Colin J. Jackson, Chris W. Coppin, et al. 2009. Catalytic Improvement and Evolution of Atrazine Chlorohydrolase. Appl. Environ. Microbiol. 75(7):2184-2191). A plasmid vector was designed for ease of purification of the enzyme with the help of a his-tag and to ensure high expression of soluble protein in recombinant *E.coli*. The specific activity and substrate specificity of the purified mutant AtzA was then compared to the wild type enzyme. It was observed from these initial studies that the mutant enzyme had somewhat similar characteristics to the wild type enzyme.

Further, the current study also describes immobilization recombinant *E. coli* cells expressing the wild type atrazine chlorohydrolase in a silica/polymer porous gel. This novel recombinant enzyme-based method utilizes both adsorption and degradation to remove atrazine from water. A combination of silica nanoparticles (Ludox TM40), alkoxides, and an organic polymer were used to synthesize a porous gel. Gel curing temperatures of 23°C or 45°C were used to either maintain cell viability or to render the cells non-viable, respectively. The enzymatic activity of the encapsulated viable and non-viable cells was high and extremely stable over the time period analyzed. At room temperature, the encapsulated non-viable cells maintained a specific activity between (0.44 ± 0.06) µmol/g-min and (0.66 ± 0.12) µmol/g-min for up to 4 months, comparing well with free, viable cells specific activities (0.61 ± 0.04 µmol/g-min). Gels cured at 45°C had excellent structural rigidity and contained few viable cells, making these gels potentially compatible with water treatment facility applications.

Table of Contents

List of Tables

List of Figures

Chapter 1: Introduction

The herbicide atrazine (2-chloro-4-ethylamine-6-isopropylamino-s-triazine) is used for control of broadleaf weeds, principally in corn, sorghum and sugarcane [1]. Atrazine is currently used in 70 countries at an estimated annual rate of 111,000 tonnes [2]. The herbicide is typically applied early in the planting season when heavy rain events may cause run-off from fields, which may result in spikes of detectable atrazine concentrations in waterways and in drinking-water supplies. This leads to municipal treatment plants having to remove atrazine along with other chemicals and odorants from drinking water. Atrazine and related triazine herbicides have been found toxic to non-target photosynthetic species, from freshwater algae to mangrove trees, as they have broad specificity [7, 8]. The half-life of atrazine in soil is significant and has been estimated at between 4 and 57 weeks, which indicates that it is not easily degraded in the environment [9]. Concentrations up to 4.6 μM of the herbicide have been detected in both surface and ground waters in several countries [10, 11, 12].

Many naturally occurring microbes have been isolated from soil for their ability to degrade atrazine. The most well studied atrazine-degrading bacterium is *Pseudomonas* sp. strain ADP. The bacterium metabolizes atrazine to carbon dioxide and ammonia via a series of six enzyme-catalyzed hydrolysis reactions [13, 14]. The genes encoding those enzymes have been sequenced and are found on a broad host-range plasmid denoted pADP1 [15]. Enzyme-catalyzed atrazine degradation is initiated by atrazine chlorohydrolase, AtzA, which hydrolytically removes the chlorine substituent from the ring and produces hydroxyatrazine (fig 1.1).

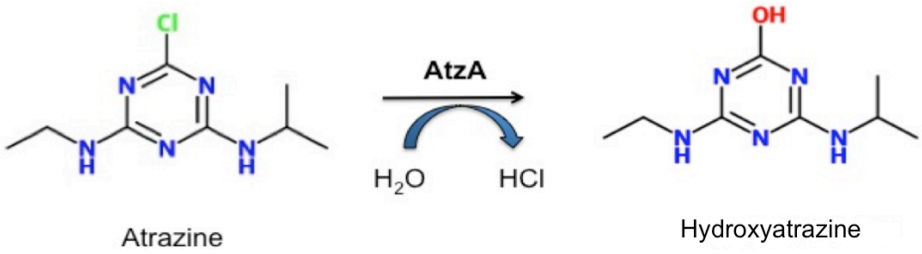

Fig 1.1: Dechlorination reaction for conversion of atrazine to hydroxy-atrazine by Atrazine chlorohydrolase

This reaction has important environmental consequences; hydroxyatrazine is not herbicidal, not as mobile in soil, and is more readily degraded than atrazine. In this context, atrazine treatments that transform atrazine to hydroxyatrazine are considered sufficient for regulatory agency approval [16].

Atrazine chlorohydrolase is a member of the amidohydrolase protein superfamily and a metalloenzyme [17]. Members of amidohydrolase superfamily have been shown to have $(\beta\alpha)_8$ barrel structure. The members of the superfamily have conserved metal binding ligands and a common hydrolytic mechanism in which nucleophilic attack on the substrate is initiated with activation of water by one or two metals present in the active site of the enzyme. Except, atrazine chlorohydrolase dechlorination is not known to be the major activity of any other member of the amidohydrolase superfamily. Though, some members of the family have been found to be capable of hydrolytic dechlorination reactions, this superfamily is most heavily represented by enzymes catalyzing hydrolysis of the amide bond and the hydrolytic displacement of amino groups from heterocyclic ring substrates. As expected from the family characteristics, AtzA has a mononuclear five-coordinate metal center that natively binds Fe(II) at the active site and is involved in activation of water molecule for nucleophilic attack.

Previous studies have shown that the chlorohydrolase gene evolved from the deaminase gene in response to the anthropogenic selection pressure induced by the widespread use of the synthetic triazine herbicide atrazine in agriculture [18, 19, 20]. Evolution of this enzyme provided a selective advantage on its host by allowing it to metabolize atrazine as a carbon and nitrogen source. The two enzymes differ from each other by only nine amino acid substitutions and the complete change in activity is particularly through a change in the Asp328- Cys331 dyad to an Asn328-Ser331 dyad [21].

The distinct catalytic dyads of these two enzymes (Asp-Cys and Asn-Ser) suited for the chemical differences between the chloride-leaving group in the chlorohydrolase and the amine-leaving group in deaminase reactions provide understanding towards the rapid change in activity on the basis of reaction mechanism. It can be reasonably assumed that activation of amine group of melamine in the deamination reaction is important for catalysis but that of the chloride group in dechlorination of atrazine is not. This

assumption is based on the fact that chloride-leaving groups are considerably more reactive than the amine leaving groups. The catalytic dyads of the two enzymes appear perfectly suited to these specific requirements. Whereas, the Asn328- Ser331 dyad of AtzA stabilizes the developing negative charge in the transition state to lower the activation energy of the reaction by hydrogen bonding of hydroxyl group of Ser331 to the leaving group which in turn would be stabilized through its hydrogen bonding interaction with Asn328. On the other hand, in the Asp328-Cys331 dyad of TriA, the aspartic acid can activate the amine-leaving group to make it more electron withdrawing and susceptible to departure by taking a proton from the cysteine and generating a thiolate. [22]

Recently, there has been a lot of interest in utilization of AtzA as both in the generation of genetically modified herbicide-resistant crops [23] and the bioremediation of atrazine contamination using recombinant microbes. Kawahigashi et al. proposed expressing mammalian cytochrome P450 in transgenic plants to phytoremediate atrazine [24, 25]. There has been interest in protein bioremediation as another option for the development of bioremediants, as it does not require the release of genetically, modified organisms in the environment. Irrespective of the method for bioremediation, there are stringent demands on an enzyme for cost-effective use as a commercial bioremediant [26, 27] and include a requirement for higher specific activity to allow removal of contaminants to concentrations below the maximum residue limits prescribed by regulatory bodies for eg. 3 ppb legal limit for drinking water in the US.

Many situations that lead to the contamination of soil, such as runoff from, or accidental spillage into them bring forth the need of biological treatment methods. This need to limit dispersion of atrazine outside of agricultural environments is the main motive behind the interests in bacterial atrazine catabolism. Strong et al. in 2000 carried out a field study using recombinant *E. coli* expressing the atrazine chlorohydrolase gene derived from *Pseudomonas* sp. ADP. A 250-gallon suspension of atrazine had been spilled onto a roadside soil leading to 900 pounds of contaminated soil, which was later on contained using a plastic liner. Some of the soil treatment options considered were: (1) removal of the soil to a landfill, (2) incineration, or (3) biological remediation. Biological degradation was found to be the cheapest treatment, and thus recombinant *E. coli* cells expressing

AtzA were treated with glutaraldehyde to chemically kill the cells and stabilize enzyme activity in soil.

The spike in atrazine levels in the environment may be caused by release in wastewater from manufacturing facilities and through its agricultural application. Due to its easy migration to ground and surface water this herbicide presents a serious threat to the local ecosystem. During the spring season there is an additional increase of atrazine concentration above the maximum contaminant level due to leaching from agricultural sources [33]. Wastewaters loaded with atrazine are usually treated with activated carbon filters, synthetic zeolites followed by advanced oxidation technologies, UV/H2O2, UV/Fenton. The total cost of these techniques is high and provide with additional problem of disposing the carbon filters and zeolites. Other methods for atrazine transformation have also been tested in the laboratory.

Entrapment of atrazine degrading bacteria in sol gels is one of the methods that have generated interest. Sol–gel processes are one of the preferred techniques and are gradually being geared towards development of thin, often multilayered, semipermeable silica matrices, somewhat like the microbes found in nature, which encompass a polymeric host with cellular activity. Immobilization of biomaterials in silica matrices was first carried out some 50 years ago. However, Braun et al. in 1990 first described properties of entrapped enzymes in TEOS-derived sol–gel matrices. In early nineties whole cell immobilization field started growing as we know it now. Carturan and his co-workers encapsulated *Saccharomyces cerevisiae*, a unicellular fungus, in sol–gel matrices. As this fungus can withstand the alcohol by-products of the alkoxide sol-gel matrix formation reactions, it was a great choice of target microorganism. Since then, several bacterial strains have successfully been immobilized in silica gels. For example, atrazine-degrading *Pseudomonas* sp. strain ADP cells have been entrapped in alginate or sol-gel glass [34]. However, significant atrazine-degrading activity was lost following encapsulation. In the methods used by the group either the proteins were denatured due to high acidity and high concentration of alcohol, or when pre-hydrolyzed TMOS was used there was rapid loss in activity of the beads in absence of a nutrient medium. To be useful in a water-treatment plant, a microbial-based treatment method should: (i) have stable, long-term atrazine-degradation activity; (ii) be mechanically stable and

sturdy; (iii) be conducive to high-water flow; (iv) maintain non-viable but active cells in the matrix without significant release, and (v) be inexpensive.

1.1 Thesis rationale and goals:

The work presented in this thesis represents a portion of research, being conducted in the Wackett Laboratory in collaboration with Biostabilization Laboratory, Department of Mechanical Engineering; that focuses on biodegradation through the use of silica encapsulated bacteria. The broad goals of this thesis were to identify an atrazine chlorohydrolase protein with higher activity and stability, and to develop a biocatalyst by silica encapsulation of whole cells expressing the protein for biodegradation of atrazine in water treatment. These studies are important for their potential to contribute to developing next generation of water treatment technology for removal of triazine ring herbicides.

1.2 Summary of thesis:

The focus of this thesis is on development of a biocatalyst for biodegradation of atrazine in water treatment systems. Chapter 2 describes a study carried out for comparison of activity and stability between the wild type enzyme and a mutant atrazine chlorohydrolase developed by Scott *et al* [22]. In our studies, the results obtained by Scott *et al.* [22] were not reproducible and we presented preliminary biochemical evidence suggesting that mutant enzyme did not have specific activity 20 times higher than that of the wild type enzyme. Chapter 3 describes silica encapsulation of *E. coli* cells expressing the wild type atrazine chlorohydrolase. The resulting silica beads were then characterized for use in water treatment systems.

Chapter 2: Expression, Purification and Biochemical Analysis of Mutant Atrazine Chlorohydrolase

2.1 Introduction:

Scott et al. [22] in 2009 proposed a recombinant protein with the active site altered to have more effective contact with the substrate to have lower K_m value. The group carried out combinatorial mutagenesis to reduce the Km of AtzA for atrazine by allowing more-productive contact with the substrate via substitution of N-isopropyl side group binding amino acids in the wild type enzyme with alternative amino acids. A combinatorial, limited site saturation library in which the amino acid residues responsible for formation of N-isopropyl side chain-binding pocket were each replaced with 1 of the 15 amino acids was made and from it the best performing mutant with proposed activity approx. 20 times the wild type enzyme was selected. Amino acid residues: alanine at 216, threonine at 217, alanine at 220, and aspartic acid at 250 in the wild type enzyme were considered to be closest to the iso-propyl side chain of the substrate and were substituted for the larger residues tyrosine, aspartic acid, histidine and glutamic acid respectively. Thus, the resulting mutant enzyme was proposed to have smaller pocket leading to closer contact between the enzyme and the substrate, resulting in the large reduction in K_m observed proposed from the kinetic analysis carried out by the group with protein fractions obtained from ammonium sulphate precipitation.

In this work, a suitable expression vector for production and purification of the mutant AtzA enzyme has been designed for comparison of biochemical characteristics with the wild type enzyme. The enzyme was his-tagged and its purification protocol optimized. Melamine deaminase (TriA) being a close homolog of AtzA is also cloned in the same vector to study the effect of his-tag on the enzyme structure. Finally, the mutant enzyme was tested for degradation of triazine ring substrates with larger side chains than atrazine to test for appreciable reduction in the size of active site of the enzyme resulting in tighter binding of atrazine as proposed by Scott *et al* [22].

2.2 Materials and methods:

2.2.1 pJS10 vector design:

The multi-cloning site from pET28b+ vector was isolated and amplified using PCR techniques with the help of appropriate primers. The PCR product was then gel purified (QIA quick gel extraction kit) and cloned into the AhdI (New England Biolabs)/ NcoI (New England Biolabs) site of pMD4 vector [14].

2.2.2 Cloning of the atrazine chlorohydrolase mutant gene:

The AtzA mutant gene was synthesized by DNA2.0 and previously cloned into a pET28b+ vector. Plasmid DNA was isolated with Qiagen's QIAprep Spin Mini prepkit. The purified plasmid was then double digested with NotI (New England Biolabs) and NcoI restriction enzymes. The 1.5 kb gene fragment was then gel purified on a 0.8% agarose and DNA extracted (QIA quick gel extraction kit). The AtzA mutant gene was cloned into the NotI and NcoI site of pMD4 containing the pET28b+ multi cloning site (Section 2.2.1), and the resulting plasmid, pJS10, was transformed into Maximum Efficiency *E. coli* DH5α (Invitrogen). The atrazine degradation phenotype of transformed cells was confirmed by incubating cell extracts with atrazine, followed by analysis using high-pressure liquid chromatography (HPLC), as previously described [28].

2.2.3 Cloning of the melamine deaminase (TriA) gene with a His-Tag:

pJS5 plasmid [29] DNA was isolated. Since, TriA and AtzA genes are 98% similar [18], a 1.1 kb fragment containing the active site all TriA specific nucleotides was isolated from pJS5 with BsshII (New England Biolabs) and BlpI (New England Biolabs) restriction enzymes. The fragment was gel purified on a 0.8% agarose gel. The purified DNA was then cloned into the BsshII and BlpI site of pJS10. The resulting plasmid was transformed into Maximum Efficiency *E. coli* DH5a (Invitrogen). The melamine degradation phenotype of transformed cells was confirmed by incubating cell extracts with melamine, followed by analysis using the Berthelot assay for ammonia detection [30].

2.2.4 *E. coli* DH5α (pMD4/pJS10) growth conditions:

E. coli DH5α cells were grown at 37°C on superbroth medium (1.2% tryptone (wt/vol), 1.4% yeast extract (wt/vol), 0.5% glycerol (vol/vol), 0.38% monobasic potassium phosphate, 1.25% dibasic potassium phosphate, chloramphenicol (30 μg/ml)). Starter cultures were obtained by inoculating 5 ml of superbroth with an isolated colony and incubating overnight. Intermediate cultures were grown by inoculation with 3% starter culture (vol/vol). Cultures were grown to an OD of 0.5-0.75 with 250 rpm. The production flasks were inoculated with 3% of the intermediate cultures (vol/vol) and grown for 16 hours under the same growth conditions. The cells were then harvested by centrifugation at 9000 rpm for 20 min at 4°C and re-suspended in phosphate buffer.

2.2.5 *E. coli* DH5α(pJS5) growth conditions:

Starter and intermediate cultures of *E. coli* DH5α(pJS5) were grown as described above. The production flasks were inoculated with 3% of the intermediate cultures (vol/vol) and induced for melamine deaminase (TriA) production with 1mM IPTG when the absorbance at 600 nm reached 0.5-1.0. The cultures are then returned to 37°C and grown for 16 hours. The cells were harvested by centrifugation at 9000 rpm for 20 min at 4 °C and re-suspended 20mM Ethanolamine, pH=9.0.

2.2.6 Expression analysis:

An isolated colony from a Luria broth (LB) chloramphenicol plate was used to inoculate 6 ml of LB chloramphenicol (30 μg/ml) media and allowed to grow to an optical density (OD) at 600 nm of 0.5. 1.5 ml of this starter culture was used to inoculate 50ml of superbroth medium with chloramphenicol (30 μg/ml). Cultures were grown overnight at 37°C with 250 rpm. At convenient time points, 5 ml samples were withdrawn and their OD was recorded. The sample was then divided to get three parts:

a) The total cell protein was then obtained by centrifuging 1 ml of the sample at 10,000 g for 60 s. The cell pellet was re-suspending in 100 μl PBS (pH=7.0). To this 100 μl of protein loading dye was added and sonicated (3

blasts of 6 sec each at 50% power) on ice. The sample was then boiled for 2-5 min and loaded on to a SDS-PAGE gel.

b) The soluble fraction was obtained by centrifuging 1 ml of the sample at 10,000 g for 60 s. The cell pellet was re-suspending in 150 μl cold 25mM Tris (pH=8.2). The sample was then sonicated (3 blasts of 6 secs each at 50% power). 100 μl of the sample were centrifuged at 14,000 g for 10 min. The supernatant was collected in a new tube and the pellet was saved for analysis of the insoluble fraction. 50 μl of protein loading dye was added to 50 μl of supernatant. The sample was then boiled for 2-5 min and loaded on to a SDS-PAGE gel.

c) The insoluble fraction was obtained by washing the cell pellet with 50 μl cold 25mM Tris (pH=8.2) thrice. Then the pellet was re-suspended in 1% SDS (wt/vol). The sample was then boiled, vortexed and sonicated. 50 μl of protein loading dye was added to 50 μl of sample and boiled for 2-5 min and loaded on to a SDS-PAGE gel.

2.2.7 SDS-PAGE:

Protein samples were loaded onto a 10% SDS-PAGE gel (FLUKA SDS Gel Preparation kit). Running buffer used was prepared by adding 3.03 g tris base, 14.4 g glycine and 1 g SDS to 1 liter distilled water.

2.2.8 FPLC purification protocol for His-trap column:

Protein was purified using His trap-chelating column. All solutions contained a base buffer of 100 mM sodium phosphate, pH 7.0. The column is generally stored in 70% ethanol when not in use. So, first the ethanol is removed by running 40ml of distilled water. Then the column is stripped of any residual protein bound to the column by removing the metal bound to the column using 0.05 M EDTA in the base buffer. The column was loaded with Co^{2+} by running 33ml of 100 mM cobalt chloride solution. The column was washed with 16 ml of the base buffer and then running 16 ml of 0.5 M imidazole through the column. The UV monitor was blanked while the high imidazole was in the flow cell. The column was equilibrated by washing the column with 40ml of the

base buffer. Valve 1 was shifted to load position and protein was loaded onto the column. The His Trap chelating column was washed with 40 ml buffer, followed by three washes of 30 ml, with 0.10 M, 0.15 M, and 0.2 M imidazole, respectively. Enzyme was eluted from the column with 30 ml of 0.25 M imidazole, which was subsequently removed from the enzyme preparation via three 4-6 h dialysis exchanges with 25 mM MOPS (pH=7.0) at 4ºC. The second exchange was supplemented with 0.5 mM iron(II) sulphate and 8 mM DTT. The dialyzed material was concentrated by ultrafiltration.

2.2.9 FPLC purification protocol for Mono-Q column:

Protein was purified using BioRad High Q Anion exchange column (15 by 118 mm). Valve 1 was shifted to load position and protein was loaded onto the column. The column was washed with 25 mM MOPS buffer (pH=7.0), and the protein was eluted using a 705-ml linear gradient of 0.0 to 0.125 M KCl in 25mM MOPS pH=7.0 at a flow rate of 1 ml/min. Protein eluting from the column was monitored at 280 nm by using a Pharmacia U.V. Protein Detector (Pharmacia, Uppsala, Sweden).

2.2.10 Purification of His-tagged protein:

Bacterial strain pJS10/TriA His-tagged was grown as described in Section 2.2.4 and were re-suspended in 100 mM phosphate buffer (pH=7.0). Protease inhibitor tablets (Roche) were added and then the cells were lysed using the French press (3 cycles, P=11000 psi). The cell lysate was centrifuged at 15000 rpm for 90 min and the supernatant (soluble fraction) was transferred to fresh tubes. The soluble fraction of protein was then loaded on to a His-column for FPLC purification using the protocol described in section 2.2.8. Fractions obtained were then analysed using SDS-PAGE (section 2.2.7) to check for protein purity. Fractions containing the protein were then dialysed with three 4-6 h dialysis exchanges with 25 mM MOPS (pH=7.0) at 4ºC. The second exchange was supplemented with 0.5 mM iron (II) sulphate and 8 mM DTT. The dialyzed material was concentrated by ultrafiltration.

2.2.11 Purification of melamine deaminase:

Bacterial strain pJS5 was grown as described in Section 2.2.5. Protease inhibitor tablets were added, and then the cells were lysed using the French press (3 cycles, P=11000 psi). The cell lysate was centrifuged at 15000 rpm for 90 min at 4 °C and the supernatant (soluble fraction) was transferred to a beaker in a styrofoam ice bucket. A 0-20% ammonium sulfate precipitation was performed over 30 min. The protein was then centrifuged at 15000 rpm for 15 min at 4 °C and pellet re-suspended in smallest possible volume of 25 mM MOPS, (pH=7.0). Re-suspended pellet containing the protein was dialyzed thrice with 4-6 h dialysis exchanges with 25 mM MOPS (pH=7.0) at 4ºC. The second exchange was supplemented with 0.5 mM Iron (II) sulphate and 8 mM DTT. The protein was then purified using protocol described in Section 2.2.9. Fractions obtained were then analyzed using SDS-PAGE (section 2.2.7) to check for protein purity. Pooled fractions containing the major peak were dialyzed thrice with 4-6 h dialysis exchanges with 25 mM MOPS (pH=7.0) at 4ºC. The second exchange was supplemented with 0.5 mM Iron (II) sulphate and 8 mM DTT. The dialyzed material was concentrated by ultrafiltration.

2.2.12 Ammonium Sulfate fraction preparation of atrazine chlorohydrolase:

Bacterial strain was grown as described in Section 2.2.4. Protease inhibitor tablets were added and then the cells were lysed using the French press (3 cycles, P=11000 psi). The cell lysate was centrifuged at 15000 rpm for 90 min at 4 °C and the supernatant (soluble fraction) was transferred to a beaker in Styrofoam ice bucket. The protein was then salted out by addition of 0-20% Ammonium sulfate to stirring supernatant over 30 min. The protein was then centrifuged at 15000 rpm for 15 min at 4 °C and pellet re-suspended in smallest possible volume of 0.1M phosphate buffer pH=7.0 [28].

2.2.13 MALDI – PMF sample preparation:

MALDI – PMF was carried out on bands observed in SDS-PAGE with the help of Todd Markowski (Assistant Scientist, Center for Mass Spectrometry and

Proteomics, University of Minnesota). The protein sample was separated with SDS-PAGE and the bands to be identified were cut out using a sharp razor blade and submitted for trypsinization and analysis.

2.2.14 BIO-RAD protein concentration assay:

Routine determinations of protein concentrations were performed with the BioRad Protein Reagent (Hercules, CA), using bovine serum albumin as a standard.

2.2.15 Atrazine decholrination activity assay:

Activity measurements of atrazine chlorohydrolase were conducted at room temperature. The reaction was initiated by the addition of 0.5 ml of 0.1 M potassium phosphate buffer (at pH 7.0) containing 150 μM atrazine to a glass tube and adding known amount of protein. The mixture was sampled at three time points (in addition to the zero) until 10 – 20% of the substrate was reacted. Each time point was taken in duplicate, and each sample was taken from an individual glass tube. The samples were boiled for 5 minutes to inactivate the enzyme and stop the reaction and filtered through a 0.2 μm pore size PTFE syringe filter. The concentrations of atrazine and its metabolite hydroxyatrazine in the sample solution were measured by High Performance Liquid Chromatography (HPLC) as previously described [14].

2.2.16 Substrate specificity assay for atrazine chlorohydrolase mutant enzyme:

Saturated solutions of the various triazine compounds listed in Table 1 were prepared in 10 mM phosphate buffer (pH 7.0). Due to the low solubility of most triazines, saturated solutions provided adequate concentrations for detection but prevented the determination of kinetic constants. The triazine solutions were incubated with 50 μl of cell extracts for 2 h at room temperature. Enzymatic reactions were stopped by heating for 2 min at 95 to 100°C. Control samples without enzyme were handled in parallel with the enzyme-treated samples. Samples were analyzed by HPLC, using a Hewlett-Packard HP 1100 system equipped with a photodiode array detector interfaced to an HP ChemStation. An adsorbosphere C18 column (250 by 4.6 mm) (Alltech,

Deerfield, Ill.) was used to separate alkylated triazines with an acetonitrile-water linear gradient as previously described [14]. An acetonitrile (ACN) gradient, in water, at a flow rate of 1.0 ml min^{-1} was used. Linear gradients of 0 to 6 min, 10 to 25% ACN; 6 to 21 min, 25 to 65% ACN; 21 to 23 min, 65 to 100% ACN; and 23 to 25 min, 100% ACN were used. Spectral data of the column eluent was collected between 200 and 400 nm at a sampling frequency of 640 ms and the spectra were referenced against a signal at 550 nm.

2.2.17 Melamine deaminase activity assay (Berthelot assay):

Activity measurements of melamine deaminase were conducted at room temperature. The reaction was initiated by the addition of 2 ml of 0.1 M potassium phosphate buffer (at pH 7.0) containing 1 mM melamine to a glass tube and adding known amount of protein. The amount of ammonia released is detected using the Berthelot reaction [30]. 0.1 ml samples are drawn from the reaction mixture at regular intervals of time and combined immediately with 0.3 ml of solution A (10g Phenol, 0.005g Sodium nitroprusside per liter of solution). Then 0.4 ml of solution B (5g Sodium hydroxide, 5.25% sodium hypochlorite per liter) is added to the mixture and vortexed. Incubate the tube for 30 minutes at room temperature and take absorbance readings at 630nm on a spectrophotometer. Ammonia reacts with phenol, nitroprusside and an alkaline solution of hypochlorite to yield indophenol, a blue chromophore, which is measured. All of the materials were purchased from Sigma (Sigma-Aldrich Corp. St. Louis, MO).

2.3 Results:

2.3.1 Cloning of pet 28b+ multi cloning site in pMD4 vector in place of the atrazine chlorohydrolase (AtzA) gene:

AtzA is currently cloned into a plasmid called pMD4. This plasmid consists of a pACYC184 backbone with a 1.4 kb insertion at the AvaI site. AtzA is expressed off of its natural promoter in this low-copy number plasmid. AtzA expression from this vector system was superior to other vectors in the level of soluble protein produced. A number of proteins in the laboratory lack successful expression in high copy number vectors like pET28b+, often producing inclusion bodies. To take advantage of the promoter and expression found in pMD4 for other proteins, the multi-cloning site with the N terminal His tag from pET28b+ was added in place of the *Atz*A gene in pMD4 to produce a new cloning vector (figure 2.1). Also, the presence of His tag in the new cloning vector makes purification of the expressed proteins much simpler than with pMD4.

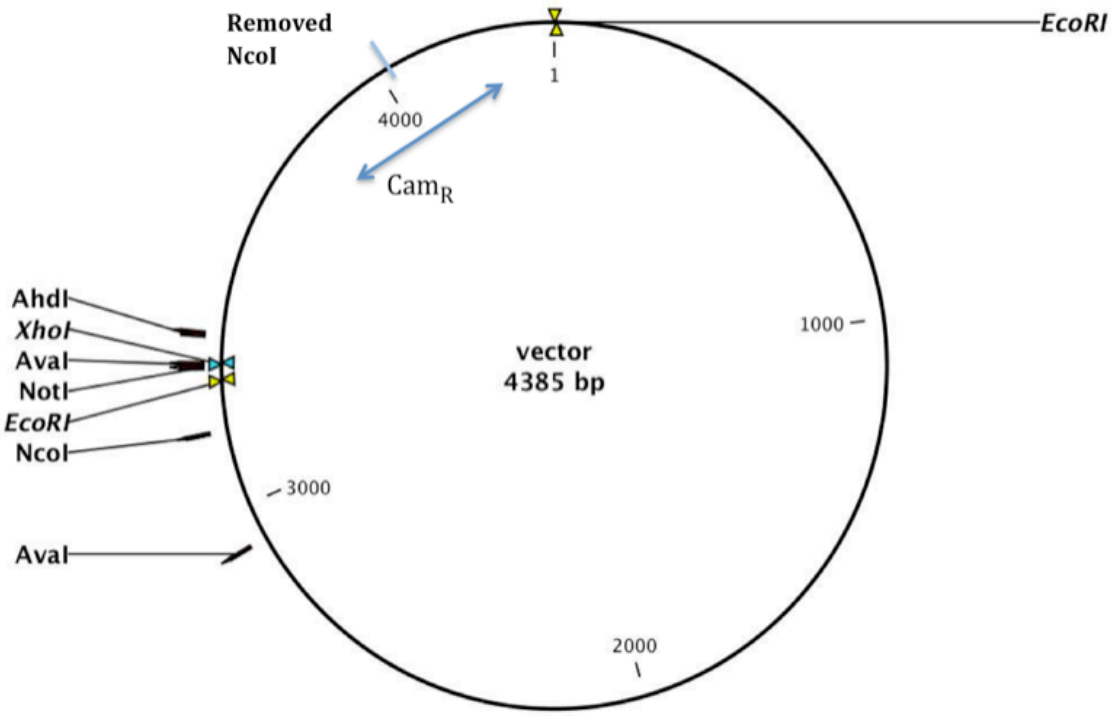

Fig 2.1: Description of the restriction sites used for designing of the modified pMD4 vector and cloning of atrazine chlorohydrolase.

2.3.2 Cloning AtzA mutant in pMD4 vector with Histag. This plasmid was named pJS10:

The AtzA protein with mutations from Scott et al. (2009) [22] was synthesized by DNA2.0 and cloned into the pET28b+ vector and resulted in inclusion body formation. This mutant protein was transferred to the pMD4 based cloning vector described in A to get higher yield of soluble protein. Successful cloning of the gene in the vector was verified by sequencing and its expression to get higher soluble protein was verified by expression analysis studies as described in section 2.2.6.

2.3.3 Cloning melamine deaminase (TriA) gene in pJS10 with Histag:

TriA is a very close homolog of AtzA. They are 98% identical in their sequence but have different functionality [18]. TriA has been expressed in nine different cloning vectors and the best one to date has modest expression. Furthermore, purification of this untagged protein is laborious. Therefore, cloning TriA into the pMD4 background with a His tag was done to improve expression and ease of purification. Additionally, this was thought of to be a good control to study the effect of His-tag on the enzyme structure and any apparent loss in activity because of the additional polypeptide. Successful cloning of the gene in the vector was verified by sequencing and its expression to get higher soluble protein was verified by expression analysis studies as described in section 2.2.6.

2.3.4 Purified His-tagged AtzA mutant activity:

Enzyme was purified using affinity chromatography on a cobalt column as described in section 2.2.10. The enzyme eluted out of the column with 0.25 M imidazole, pH=7.0. The yield obtained was 13.5 – 15 mg of enzyme per liter of culture. Fractions containing the enzyme observed from the peak on the chromatogram (figure 2.2) were analyzed with SDS- PAGE before pooling them together and dialysis. The protein showed a doublet on the SDS-PAGE, which was then further, analyzed using MALDI – PMF. Search results obtained from Mascot database confirmed that both the bands were atrazine

chlorohydrolase protein with protein scores of 143 and 190 respectively (83 is considered to be the significant score for protein identification). The MALDI-PMF analysis was done with the help of Todd Markowski (Assistant Scientist, Center for Mass Spectrometry and Proteomics, University of Minnesota).

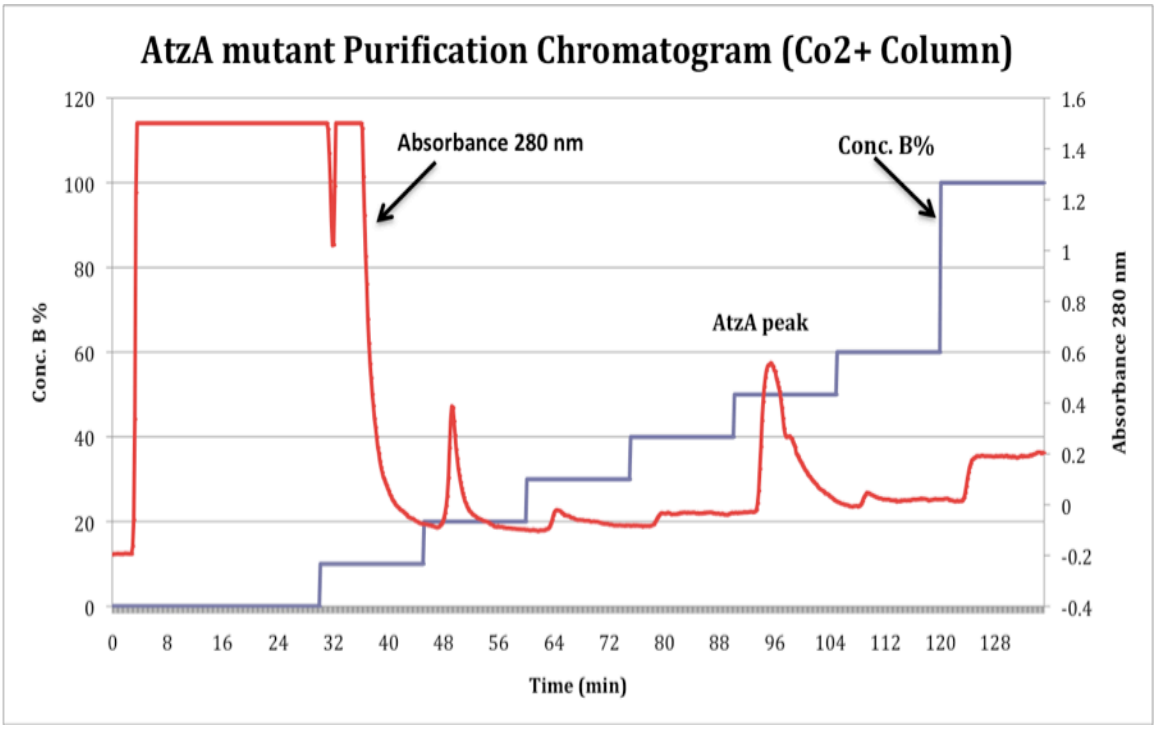

Fig 2.2: Chromatogram for purification of atrazine chlorohydrolase mutant enzyme on a Co^{2+} column.

The specific activity observed was in the range 2.1 – 3.9 μmol/ mg-min and was calculated by using the atrazine dechlorination activity assay as described in section 2.2.15. This activity was calculated on the basis of protein concentrations calculated on the basis of total protein concentration of fractions obtained from the FPLC calculated with Bio-rad protein assay and considering BSA (Bovine Serum Albumin) as standard and the standard curve generated by plotting peak areas of different concentrations of atrazine (figure 2.3).

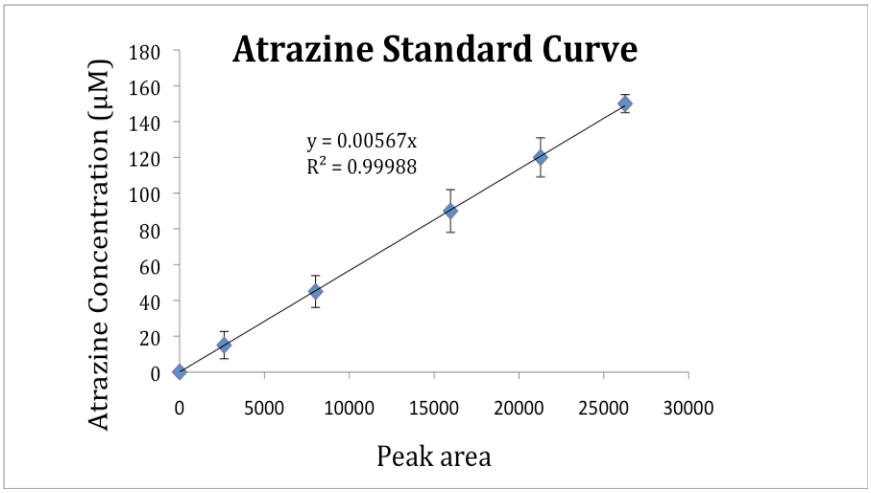

Fig 2.3: Standard curve for atrazine concentration vs. peak area for HPLC analysis

The specific activity calculations were made on the basis of atrazine turnover rate calculated by analyzing samples drawn from the reaction mixture at regular intervals of time on HPLC as shown in the figure 2.4.

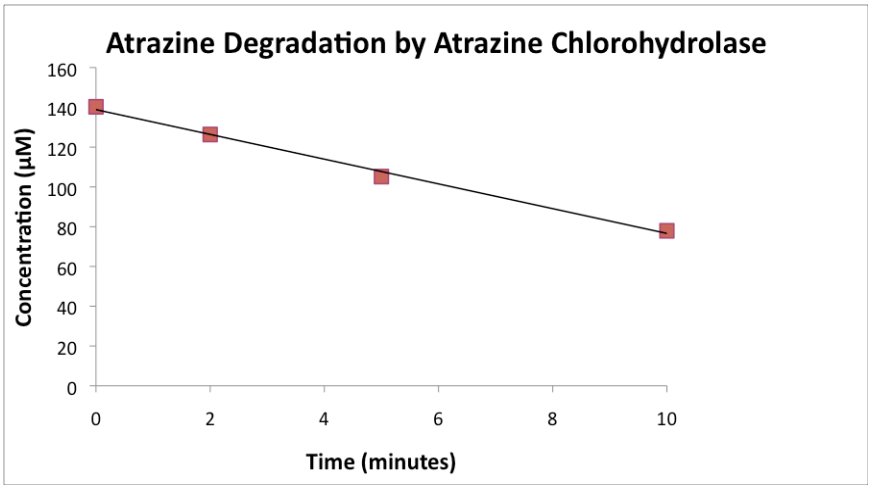

Fig 2.4: Atrazine chlorohydrolase activity assay chart depicting concentration of atrazine with time.

Specific activity calculation for mutant enzyme is shown below:

Atrazine turnover rate = 7.01 μmol L^{-1} min^{-1}

Mass of Protein = 0.09 mg

Reaction volume = 0.005 L

Specific Activity = (Atrazine turnover rate)(Reaction volume)/(Mass)

Enzyme Sample	Specific Activity (µmol/mg-min)
Mutant AtzA	3.89
Wild Type AtzA	3.86

Table 2.1: Table depicting comparison of observed specific activity values of mutant AtzA to that of the wild type enzyme.

Additionally, when the purified enzyme sample was analyzed using Gel – Densitometry (figure 2.5) which uses a much more sensitive silver staining. It was observed that the percentage of AtzA was only 30% of the total protein in the sample. Same sample when tested with SDS-PAGE showed a single band on the gel. Hence, the observed specific activity with gel densitometry i.e. 12.96 μmol/ mg-min, was higher than the one observed with Biorad Assay and SDS- PAGE.

a)

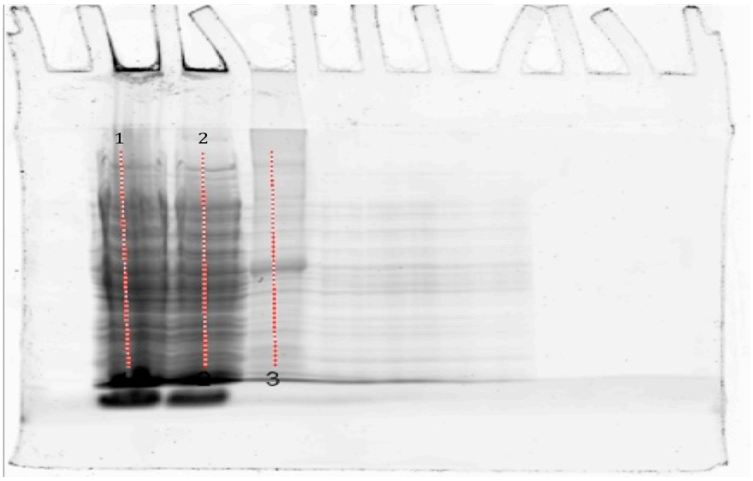

b)

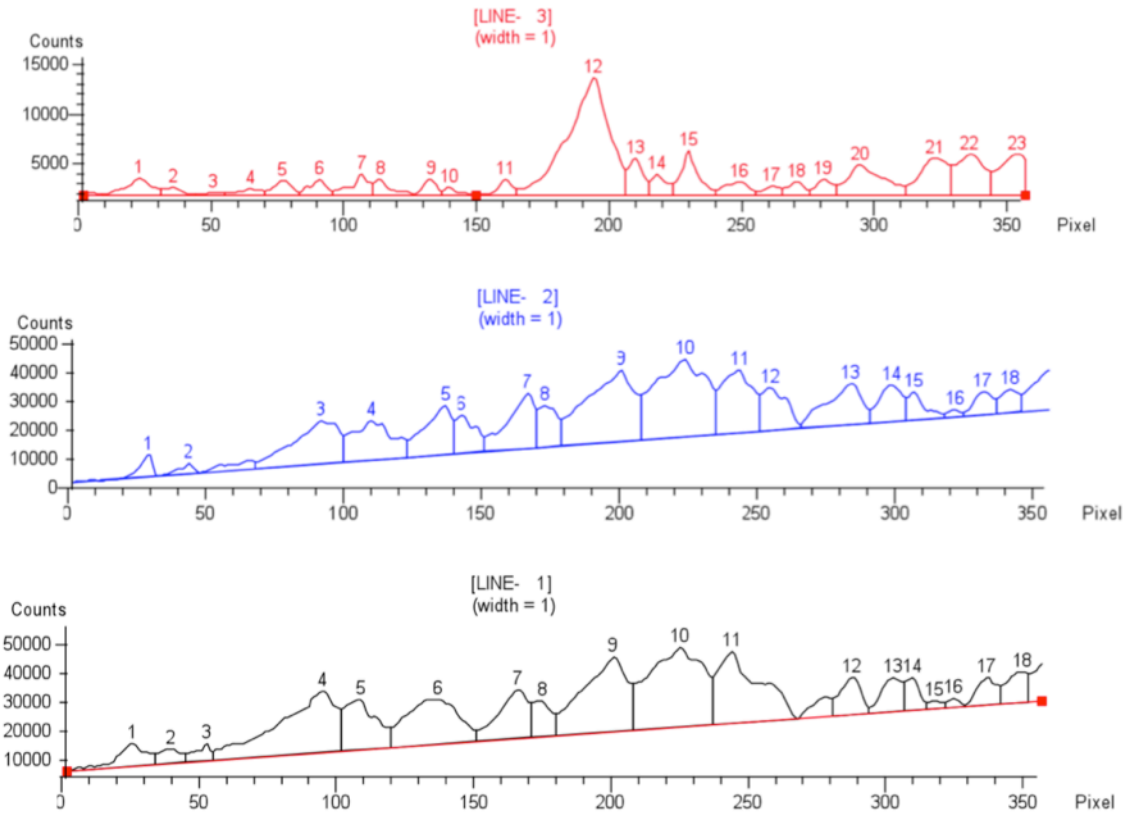

Fig 2.5: Figure shows the gel densitometry data for the protein expression in *E. coli*. a) The gel in the image has been stained using the silver staining. Lines 1, 2, and 3 are cell lysate 1, cell lysate 2 and purified enzyme respectively. b) Shows the densitometry analysis data of various bands on the gel. The peak around 200 pixel represents the protein AtzA on gel.

2.3.5 Purified wild type and His-tagged TriA mutant activity:

The wild type enzyme (strain pJS5) was purified using anion exchange chromatography as described in section 2.2.11 and the his-tagged enzyme was purified using affinity chromatography on a cobalt column as described in section 2.2.10. Fractions containing the enzyme observed from the peak on the chromatogram (fig 2.8) were analyzed with SDS- PAGE before pooling them together and dialysis. The specific activity was calculated using the berthelot assay as described in section 2.2.17. The standard curve generated by plotting peak areas of different concentrations of Ammonium chloride (figure 2.6).

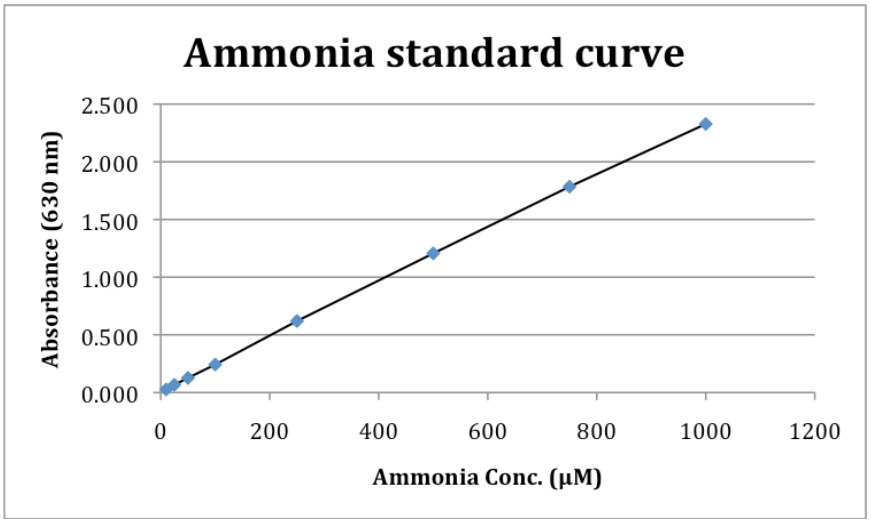

Fig 2.6: Standard curve for absorbance (630 nm) vs. ammonia conc. for spectrophotometer analysis. Error bars are smaller than the data points.

100 µl samples were obtained after incubation with both histagged (4 µg/ml) and untagged enzyme (5 µg/ml) at regular intervals of time and analyzed for ammonia concentration (figure 2.7).

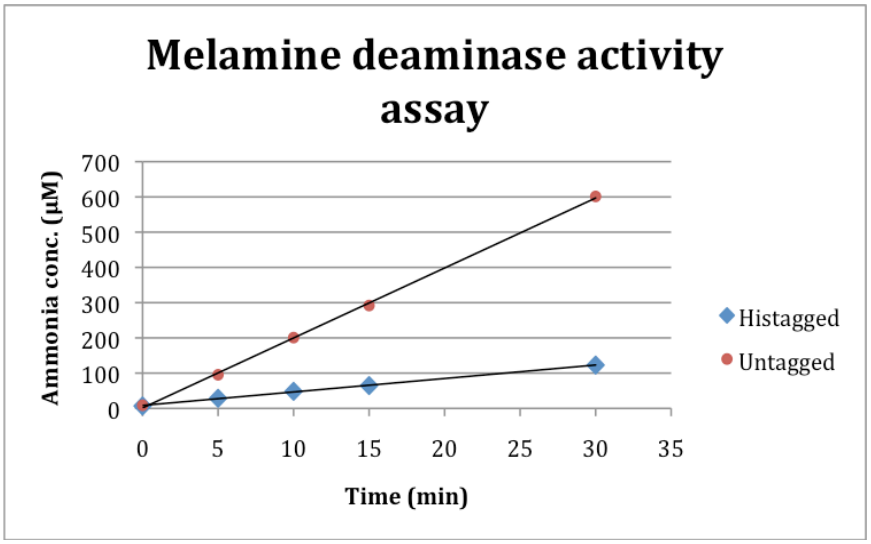

Fig 2.7: Melamine deaminase activity assay chart depicting ammonia release from the reaction with time in the presence of histagged and untagged enzyme.

Histagged Enzyme:

Ammonia production rate = 3.930 μmol L^{-1} min^{-1}

Mass of Protein = 0.008 mg

Reaction volume = 0.002 L

Specific Activity = (Atrazine turnover rate)(Reaction volume)/(Mass)

Untagged Enzyme:

Ammonia production rate = 21.085 μmol L^{-1} min^{-1}

Mass of Protein = 0.010 mg

Reaction volume = 0.002 L

Specific Activity = (Atrazine turnover rate)(Reaction volume)/(Mass)

The specific activity observed for histagged enzyme was 0.98 μmol/mg-min. The purified his-tagged enzyme had approximately 4 times lower specific activity then the untagged wild type enzyme (4.2 μmol/ mg-min). The decrease in activity indicates disliking of the enzyme structure for the his-tag. This was considered to be a vital observation also for atrazine chlorohydrolase because of the sequence homology.

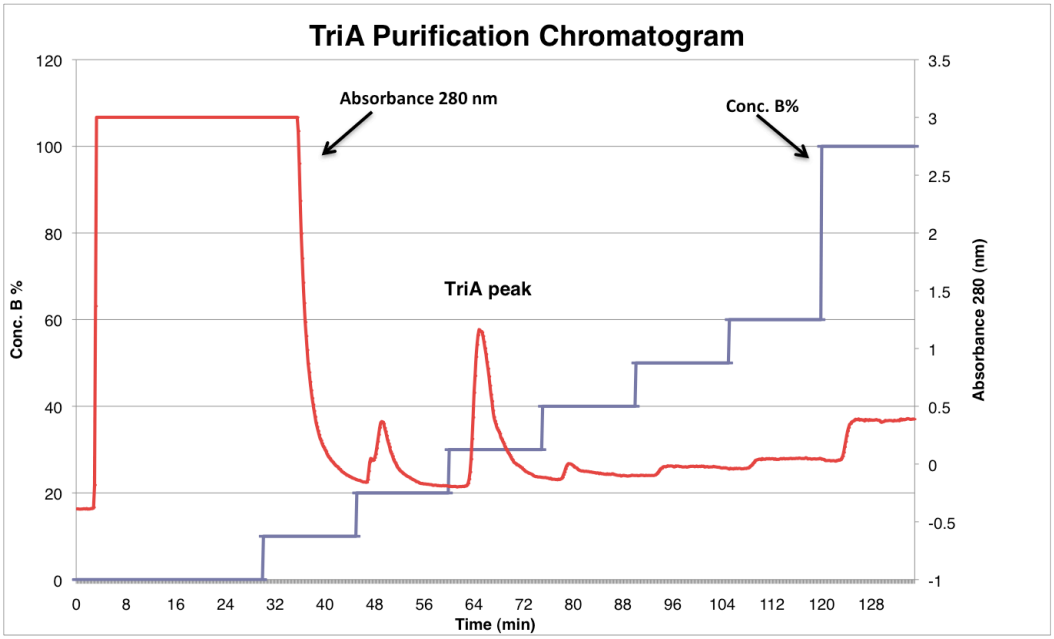

Fig 2.8: Chromatogram for purification of his-tagged melamine deaminase enzyme on a Co^{2+} column.

2.3.6 Purified AtzA mutant substrate specificity:

The substrate specificity assay was carried out as described in section 2.2.16 with substrates: 2-Chloro-4,6-di(N-isobutylamino)-1,3,5-s-triazine, 2-Chloro-4,6-di(N-sec-butylamino)-1,3,5-s-triazine, 2-Chloro-6-(N-t-butylamino)-4-(N-ethylamino)-1,3,5-s-triazine. Triazine substrates for this study were synthesized by Gilbert Johnson and were analyzed by gas chromatography mass spectrometry (GC-MS) using an HP 6890/5973 instrument (Hewlett-Packard, San Fernando, Calif.) [31]. These substrates have side chains bigger than that present in atrazine. The atrazine chlorohydrolase mutant was designed such that larger residues were substituted for the wild-type amino acids (A216Y, T217D, A220H, and D250E) in the binding site to result in closer contacts between the enzyme and atrazine leading to a reduction in the K_m value of the enzyme. But, the mutant enzyme was still able to catalyze the dechlorination of these substrates with considerably bigger side chains than atrazine. The degradation of these substrates 2-Chloro-4,6-di(N-isobutylamino)-1,3,5-s-triazine, 2-Chloro-4,6-di(N-sec-butylamino)-1,3,5-s-triazine, 2-Chloro-6-(N-t-butylamino)-4-(N-ethylamino)-1,3,5-s-triazine by the mutant atrazine chlorohydrolase can be observed from the chromatograms in fig 2.9, 2.10 and 2.11 respectively. Hence, the reduction in size of the isopropyl binding pocket was not observed when tested with the bigger butyl side groups.

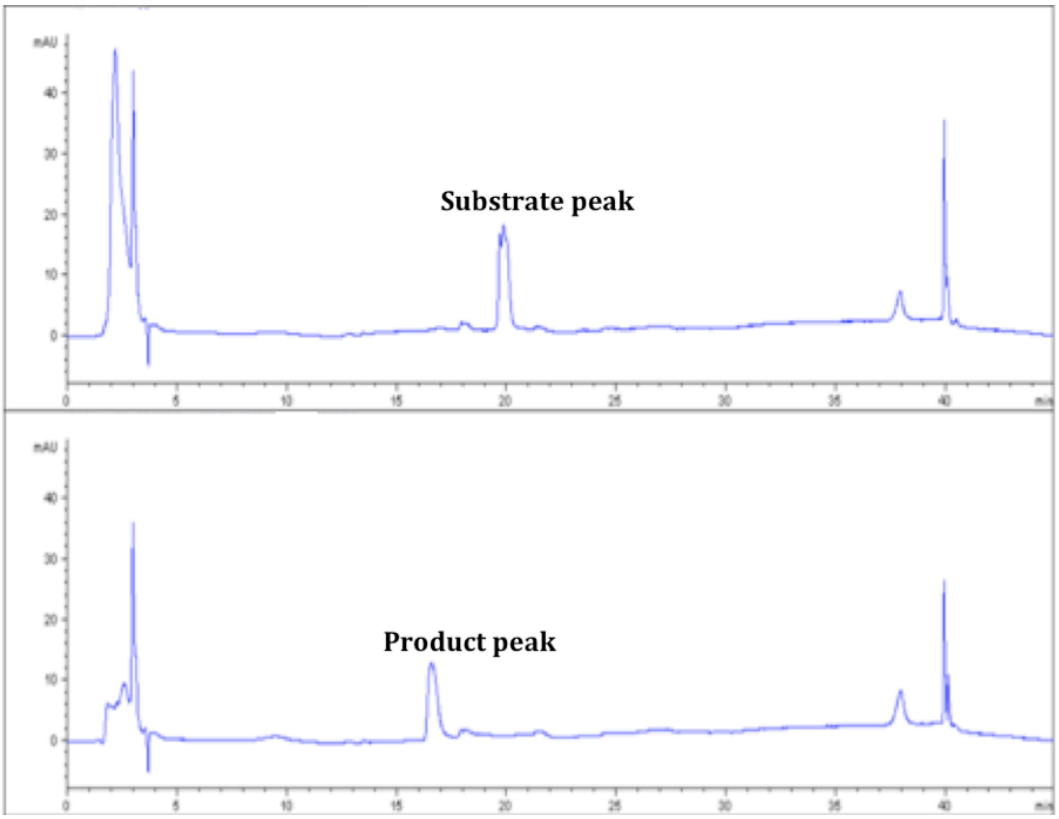

Fig 2.9: Chromatogram depicting degradation of 2-Chloro-4,6-di(N-isobutylamino)-1,3,5-s-triazine on incubation with mutant atrazine chlorohydrolase.

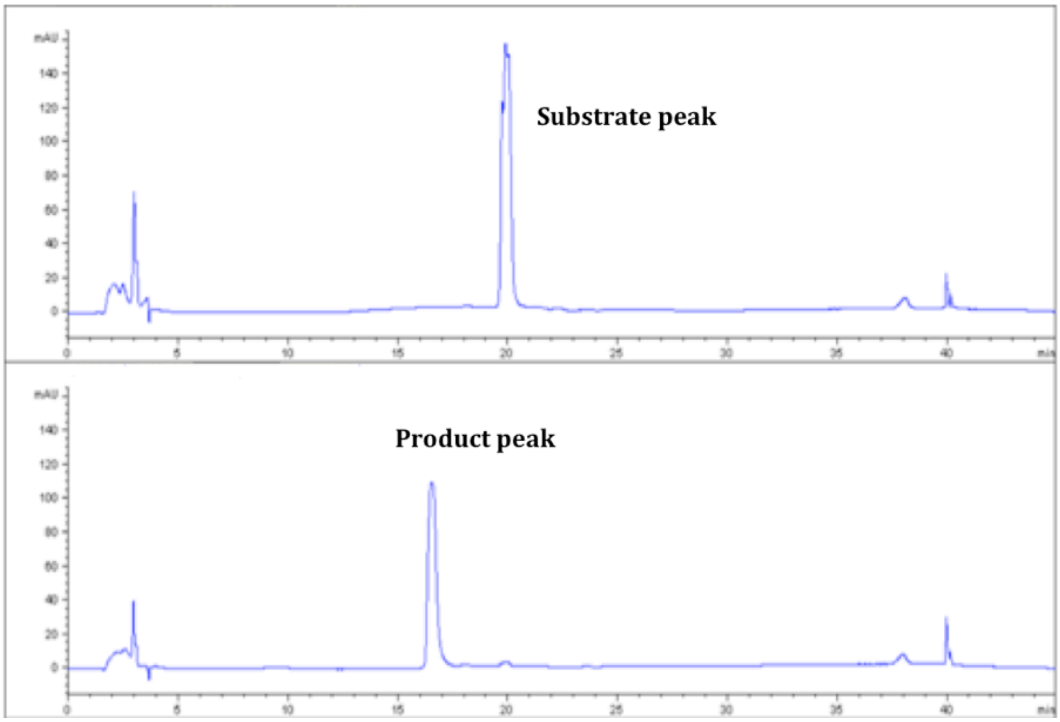

Fig 2.10: Chromatogram depicting degradation of 2-Chloro-4,6-di(N-sec-butylamino)-1,3,5-s-triazine on incubation with mutant atrazine chlorohydrolase.

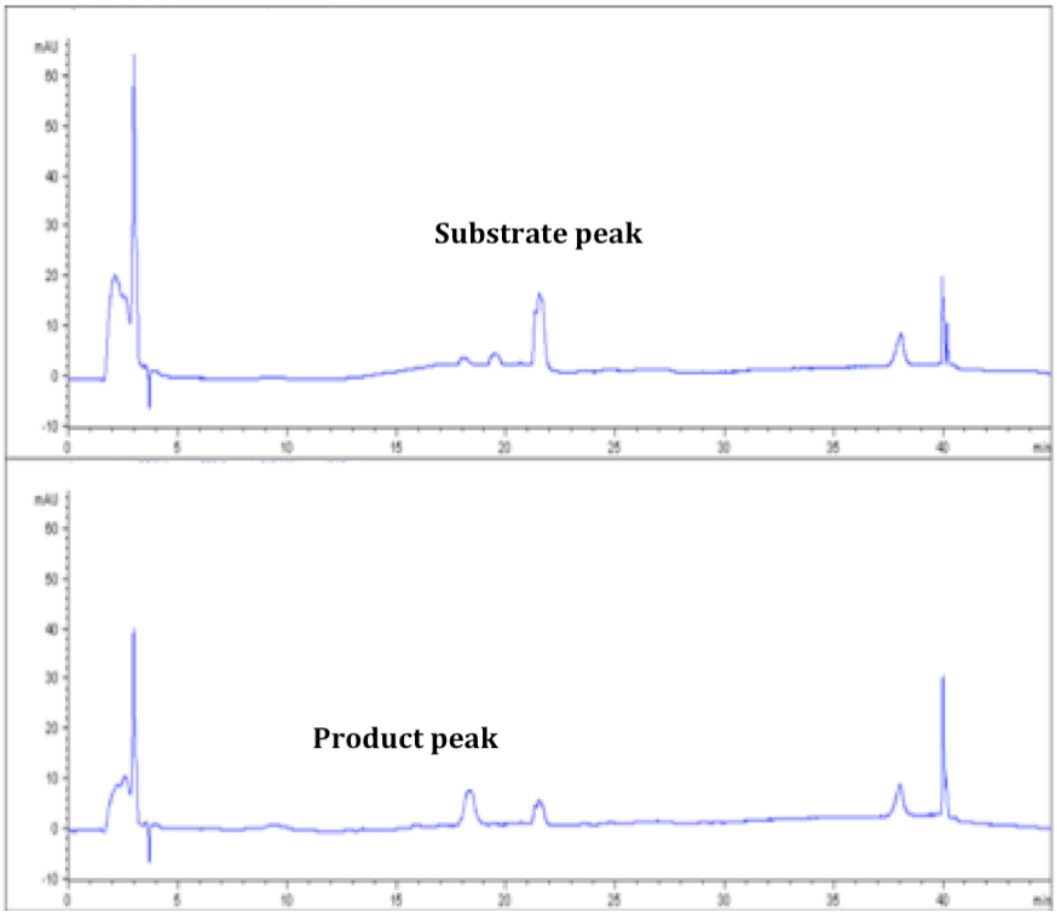

Fig 2.11: Chromatogram depicting degradation of 2-Chloro-6-(N-t-butylamino)-4-(N-ethylamino)-1,3,5-s-triazine on incubation with mutant atrazine chlorohydrolase.

2.4 Discussion:

There has been increasing interest in improving the biochemical characteristics of atrazine chlorohydrolase with realization of its widespread application in various strategies for biodegradation of atrazine. In this study along with development of purification strategy for the mutant AtzA we tried to better understand the effect of mutations carried out by Scott *et al* [22].

2.4.1 Cloning and purification of atrazine chlorohydrolase and melamine deaminase:

Both enzymes were successfully cloned under a strong constitutive promoter in a low copy number plasmid and with a his-tag. Enzymes were expressed well in the plasmid resulting in high yield of soluble protein. The his-tag allowed for a simple and efficient purification protocol resulting in higher yields of purified protein than with previously used anion exchange column. The activity of mutant atrazine chlorohydrolase observed was in the same range as that of the wild type enzyme reported previously [28]. The activity when calculated on the basis of gel densitometry results which uses a much more sensitive silver stain was found to be thrice the activity calculated on the basis of Bio-Rad assay dependent protein values. Though, the observed activity values of his-tagged melamine deaminase were lower than without the his-tag. Hence, further studies are required to check the compatibility of his-tag with $(\beta\alpha)_8$ barrel structure of atrazine chlorohydrolase.

2.4.2 Atrazine chlorohydrolase turnover number:

The mutant enzyme was developed to have higher K_{cat} with atrazine by Scott *et al* [22]. In this study, when calculations for the parameter was made based on the specific activity observed for the purified protein using Michaelis-Menten kinetics:

Where, $$v = \frac{V_{\max}[S]}{K_m + [S]}.$$

Now as the enzyme concentration in the reaction is much lower than the substrate concentration as the enzyme concentration used for mutant is 73.5

nM and 53.06 nM for the wild type whereas the starting substrate concentration in the reaction is 150 µM.

$$V_{max} = k_{cat}[E]_0$$

Which implies,

$$k_{cat} = V_{max}/[E]_0$$

$$k_{cat} = V_{max}(M_w)/(\text{Amount of protein})$$

We know, Specific Activity (SA)= V_{max}/(Amount of protein)

Hence, $k_{cat} = (SA)(M_w)$

The molecular weight (M_w)= 245 KDa as reported previously[28].

Using the specific activity values from the results section (Table 2.1) and the above equations for k_{cat} and V_{max} we get

Enzyme sample	K_{cat} value (sec^{-1})		Vmax (µmol/sec)
	Published	Observed	Observed
Mutant AtzA	27.9	15.9	1.168
Wild Type AtzA	16.1	15.8	0.838

Table 2.2: Table depicting comparison of observed K_{cat} values of mutant AtzA to that of the wild type enzyme and the observed Vmax values.

Hence, it was observed that the observed value of K_{cat} for the mutant enzyme was way lower than that of the published value [22] and was in the same range as the value observed for the wild type enzyme [17].

2.4.3 Atrazine chlorohydrolase substrate specificity:

We tried to test the reduction in size of the active site by incubating the enzyme with substrates having bigger butyl groups on the side chain as compared to isopropyl and ethyl groups present in atrazine. These substrates have previously been reported, to be metabolized by the wild type enzyme [31]. The purpose was to check for a considerable decrease in the size of the isopropyl side chain binding pocket of the active site, which could explain the reduction in K_m value for the enzyme. The three substrates used are shown in figure 2.9 along with the structure of atrazine molecule. Enzyme kinetic studies could not be carried out for these because of their low solubility in water. But, the enzyme was able to catabolize the substrates, which indicates that the substrate was able to bind to the active site inspite of, the decrease in size of the site. Hence, further studies with larger side groups along with kinetic analysis of the purified enzyme could prove to be insightful in knowing more about the active site structure of the mutant enzyme.

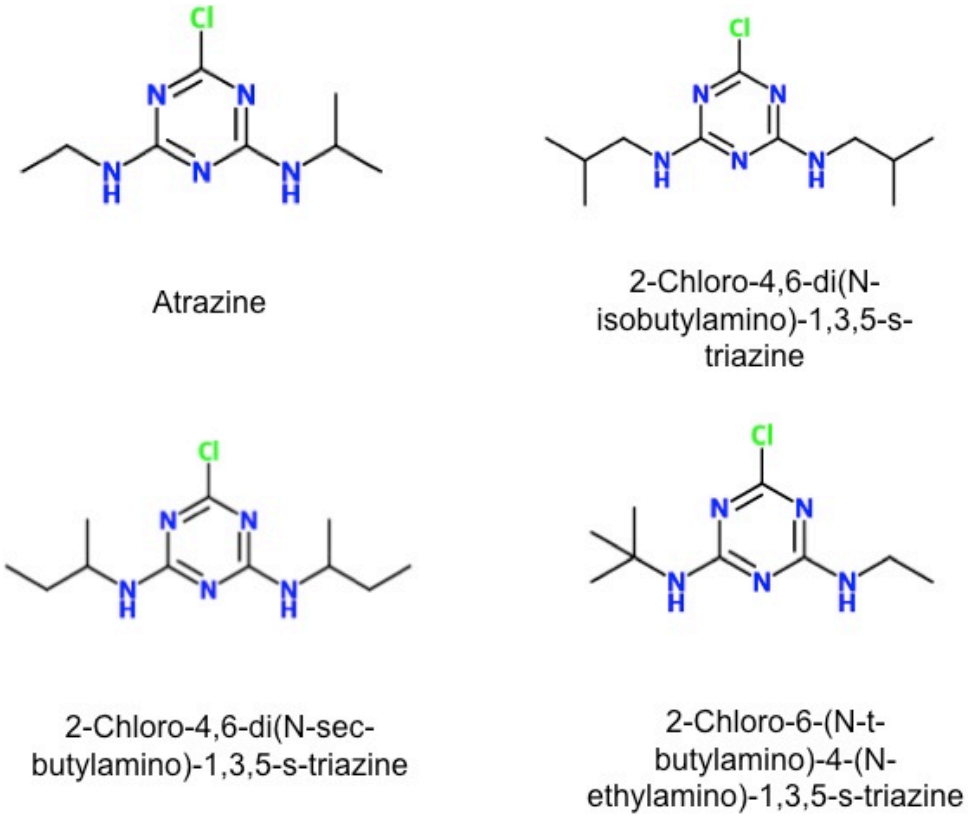

Fig. 2.12: Structure of substrates used in substrate specificity study. It should be noted that all the candidates used have a bigger side chain than the isopropyl side chain of atrazine.

Chapter 3: Silica Gel Encapsulation of Recombinant *E.coli* Cells Expressing AtzA for the Biodegradation of Atrazine into Hydroxyatrazine

Disclaimer: This Chapter is similar to the work in the paper Eduardo Reátegui, Erik Reynolds, Lisa Kasinkas, Amit Aggarwal, Mike J. Sadowsky, Alptekin Aksan, Larry P. Wackett, Silica Gel Encapsulation of Recombinant *E.coli* Cells Expressing AtzA for the Biodegradation of Atrazine into Hydroxyatrazine, Journal for Applied microbiology and biotechnology (in press). My role in the project was growing the *E.coli* strain, testing for enzyme activity, permeabilizing treatments and cell viability assays.

3.1 Introduction:

In this study, in collaboration with *Biostabilization laboratory, Department of Mechanical Engineering, University of Minnesota*, we developed a hybrid biomaterial to be used for atrazine biodegradation that meets the requirements for use in municipal water-treatment facilities. The biomaterial consisted of recombinant *E. coli* cells over expressing atrazine chlorohydrolase (AtzA) encapsulated in a polymer/silicon oxide matrix prepared by the sol-gel process. The gelation process was conducted through mild chemical reactions, thus overcoming previously described problems of loss of enzyme activity over time. Pre - hydrolysis of metal alkoxide (TMOS) precursors was carried out resulting in the formation of silanol groups (Si-OH); through condensation, these silanol moieties were reacted further to form siloxanes (Si-O-Si); finally through polycondensation of silanol and siloxanes, SiO2 matrices are formed after aging and drying processes [35].

$$(RO)3SiOR + H2O \rightarrow (RO)3SiOH + ROH \quad [1]$$
$$2(RO)3SiOH \rightarrow (RO)3Si\text{-}O\text{-}Si(OR)3 + H2O \quad [2]$$
$$(RO)3SiOH + ROSi(OR)3 \rightarrow (RO)3Si\text{-}O\text{-}Si(RO)3 + ROH \quad [3]$$

Moreover, conditions were developed that led to non-viable cells that remained fully active in degrading atrazine over long time scale. The silica base matrix encapsulating the microorganisms consisted of a combination of silicon oxide precursors (e.g., silica nanoparticles, alkoxides) and a biocompatible organic polymer (e.g., polyethylene glycol, PEG). The porous material enabled diffusion of water and atrazine into the gel, and diffusion of hydroxatrazine out of the gel. The material had the additional advantage of stability over calcium alginate encapsulated bacteria, which showed good activity but the beads showed swelling and eventually developed cracks [34]. The gel also adsorbed atrazine, a property that contributed to removal of atrazine from the solution in the process. In this context, the material we developed performed significantly better than activated charcoal since it both adsorbed and then degraded the herbicide. As shown here, the final material exhibited uniform catabolic activity for four months. In total, these studies indicated

that the described hybrid biomaterial could be used continuously for the degradation of atrazine without the need for regeneration.

3.2 Materials and methods:

3.2.1 Silica gel material:

The matrix used is the one described by Reatgui *et al.* [36] in the *Biostabilization laboratory, Department of Mechanical Engineering, University of Minnesota*. The gel consisted of colloidal silica nanoparticles Ludox TM40 (40% w/w), tetramethyl orthosilicate (TMOS, 98%), and methyltrimethoxy silane (MTMOS, 97%). The organic polymer, polyethylene glycol (PEG, molecular weight (M_w): 600 Da), was incorporated into the porous matrix in order to increase biocompatibility of the matrix. All of the materials were purchased from Sigma (Sigma-Aldrich Corp. St. Louis, MO).

3.2.2 Bacterial strains and growth conditions:

E. coli DH5α (pMD4) [14] was grown at 37°C in superbroth medium comprised of 1.2 % tryptone (w/v), 1.4 % yeast extract (w/v), 0.5 % glycerol (v/v), 0.38 % monobasic potassium phosphate, 1.25 % dibasic potassium phosphate, and 30 μg/ml chloramphenicol (at pH 7.4). Starter cultures were made by inoculating 5 ml of superbroth with an isolated colony and incubating overnight at 37°C, with shaking at 250 rpm. Intermediate cultures were grown by inoculation with 3 % (v/v) starter culture. Cultures were grown to an optical density (OD) of 0.5 - 0.75 with shaking at 250 rpm. Cell production flasks were inoculated with 3 % (v/v) of intermediate cultures and grown for 16 h under the same growth conditions. Cells were harvested by centrifugation at 9000 rpm for 20 min at 4°C and re-suspended in water to a final concentration of 0.1 - 0.2 g of cell/ml.

3.2.3 Reactive biomaterial production:

Bacterial cells were encapsulated using sol-gel method previously described [36] in the *Biostabilization laboratory, Department of Mechanical Engineering, University of Minnesota*. Cells were encapsulated in silica or silica-PEG (SPEG) gels. Porous gels were formed by diluting TM40 silica nanoparticles in ultra pure water (with electrical resistivity > 18.2 MΩ.cm at 25°C). PEG (M_w = 600 Da) was added to the solution at a volume ratio of 1:4 (r_{PEG}), and the mixture

was stirred vigorously for 10 min. The resulting TM40-PEG solution was cooled in an ice bath. Separately, TMOS or TMOS/MTMOS were hydrolyzed by sonication in the presence of 0.01 M HCl. A typical volume ratio was 1:1:0.1 for TMOS/water/HCl and 1:1:1.5:0.15 for the TMOS/MTMOS/water/HCl solution. The hydrolyzed solution was mixed with the TM40-PEG solution at a volume ratio of 1:2 (r_{cl}). Finally, a cell suspension (0.1 or 0.2 g of cells /ml) was added to the mixture at a volume ratio of 1:1 (r_{cs}). Gels for formed in two different conformations i.e. cylindrical block and microbeads. The cylindrical block was formed by pipetting 1 ml of the liquid formulation described above in a glass scintillation vial and allowing it to polymerize and hence encapsulating the cells in the matrix for 90 min at 23°C on the workbench. The final dimensions of the cylindrical plug formed were diameter of approximately 25 mm and a thickness 2 mm. The microbeads (1.0 - 1.5 mm diameter) were formed by casting 65 ml of the mixture in a metal mold and incubating at 23°C and 45°C for 24 hours in a convection oven for polymerization of silica encapsulating the cells present in the mixture. The final gels were weighed to observe 4% cells by weight in the gels which were formed by using 0.1 g cells /ml in the initial mixture and 8% cells by weight in the gels which were formed by using 0.2 g of cells/ml in the initial mixture.

Table 3.1 Composition of silica gels

Gel Type	Precursor	PEG	Cross-linker		*E. coli* cells		Incubation
	[M]	r_{PEG} [v/v]	Type	r_{cl} [v/v]	r_{cs} [v/v]	[g of cell/ml]	[°C]
N1	1.24	-	I	0.5	1	0.1	23
N2	1.13	0.25	I	0.5	1	0.1	23
N3[a]	1.13	0.25	I	0.5	1	0.1	23
N4[b]	1.13	0.25	I	0.5	1	-	23
N5	1.71	0.25	II	0.5	1	0.1 or 0.2	23 or 45

[a] *E. coli* non-expressing AtzA

[b] No cells

I: TMOS:Water:0.01M HCL (1:1:0.1 v/v/v)

II: TMOS:MTMOS:Water:0.01M HCL (1:1:1.5:0.15 v/v/v/v)

r_{PEG} = volume of PEG / volume of precursor

r_{cl} = volume of cross-linker / volume of precursor

r_{cs} = volume of cell solution / volume of precursor

3.2.4 Viability assay:

The plate-count assay was used to determine cell viability of gel-encapsulated cells. A 0.1 g aliquot (wet weight) of gel was pulverized by gentle compression between two glass slides to release the encapsulated *E. coli*, as previously reported [37]. The crushed material was suspended in 3 ml of sterile phosphate buffered saline (PBS). The solution was serially diluted and spread-plated, in triplicate, onto Luria Broth agar plates [38]. In the case of oven-treated N5 gels, serial dilutions were not used and 400 μl of the 3 ml crushed gel suspension was directly plated. Plates were incubated at 37°C for 24 h and mean colony forming units (CFU) per gram of gel are presented.

3.2.5 Lipid membrane analysis of encapsulated cells:

Conformation of cellular membrane lipids was characterized using Fourier Transform Infrared (FTIR) spectroscopy by Eduardo Reatgui and Lisa Kasinkas at *Biostabilization laboratory, Department of Mechanical Engineering, University of Minnesota*. Before gelation, 0.5 μL of the cell sample was sandwiched between two CaF_2 windows that were separated by a thin layer of vacuum grease on the sides and placed on a temperature control cryostage (FDCS 196, Linkam Scientific Instruments Ltd., UK). FTIR spectra were collected in the 930 – 7000 cm^{-1} range using a Nicollet Continuμm FTIR microscope, equipped with a DTGS detector (Thermo-Nicollet Corp., Madison, WI). FTIR spectra were collected at 4, 10, 23, and 37°C. Spectral analysis was performed using Omnic software provided by the manufacturer. The lipid conformation change in the cellular membranes was monitored by measuring the peak location of the ν-CH_2 (symmetric stretching) band located near 2850 cm^{-1}. Due to significant contributions of the PEG CH_2 chains in the 2700-3000 cm^{-1} region of the IR spectra, only silica gels without PEG were used for the analysis.

3.2.6 Membrane permeabilization of *E.coli*:

Bacterial strain pMD4 was grown as described in section 2.2.4. Acetone and Triton X-100 were selected as the best candidates for permeabilization as

previously described [39]. 10ml of resuspended cells are then taken in two tubes A and B. Cells in tube A are incubated with 10% Acetone (v/v) for 10 minutes at 4°C and cells in tube B are incubated with 2% Triton X-100 (v/v) for 10 minutes at room temperature. Cells are then pelleted with the help of a bench top centrifuge at 6000 rpm and 4°C. The supernatant is saved to analyze for protein release using SDS-PAGE and the Bio-rad assay as described in section 2.2.7 and 2.2.14. The pelleted cells are washed by 2 cycles of resuspending in 0.1 M PBS and pelleting. Finally, the cells are resuspended in 100 mM phosphate buffer (pH=7.0) for dechlorination activity assay as described in section 2.2.8.

3.2.7 Effect of various additives on activity of *E. coli*:

Bacterial strain pMD4 was grown as described in section 2.2.4. Eight tubes containing 5ml each of the resuspended cells were incubated for 30 minutes with no additive as control, 5% Polyethylene glycol (PEG), 10% PEG, 5% Trehalose, 10% Trehalose, 20% Trehalose, 5% Pluronic F-127 **(**P127) and 10% P127 (Sigma-Aldrich Corp. St. Louis, MO) respectively. Then known amount of cells are obtained for dechlorination activity assay as described in section 2.2.8. The concentration of additives was maintained in the reaction mixture. At the end of the experiment OD600 values were compared to initial OD values with the additives to check for cell lysis if any.

3.2.8 Atrazine dechlorination activity assay for immobilized enzyme:

Activity measurements of the encapsulated cells, in a cylinder block or in microbead form, were conducted at room temperature and at 4°C in 20 ml glass scintillation vials. The reaction was initiated by exposing the cylinder block on one surface to 5 ml of 0.1 M potassium phosphate buffer (at pH 7.0) containing 150 μM (32.4 ppm) atrazine. In the experiments conducted with microbeads, 100 microbeads were suspended in 5 ml of the same solution used for the cylinder blocks. The solution was continuously stirred using an orbital shaker at 200 rpm. The supernatant was sampled at four time points until 10 - 20 % of the substrate was reacted. Each time point was taken in

duplicate, and each sample was taken from an individual scintillation vial. The samples were heated to boiling point for 5 min to ensure that any released enzyme was inactivated, and filtered through a 0.2 μm pore size PTFE syringe filter to remove any bead fragments or cells that may have been released. The concentrations of atrazine and its metabolite, hydroxyatrazine, in the sample solution were measured by High-Performance Liquid Chromatography (HPLC) as previously described [14]. For long-term activity measurements, the encapsulated and free cells were stored in water at 4°C and assayed as described above.

3.2.9 Characterization of the porous gel:

The study was carried out by Eduardo Reátegui **(***Biostabilization laboratory, Department of Mechanical Engineering, University of Minnesota).* For electron microscopy imaging, silica or SPEG gels that contained encapsulated bacteria were chemically fixed initially using 2 % glutaraldehyde, and then 1 % osmium tetraoxide diluted in 0.1 M sodium cacodylate. After fixation, samples were gradually dehydrated by exposure to 50, 70, 80, 95, and 100 % ethanol. The samples were then transferred to a CO_2 critical point drier (Samdri-780A, Tousimis, Rockville, MD). Dried samples were sputtered with tungsten at a rate of 1 A°/min for 10 min. The gels that did not contain bacteria were sputtered without fixation. Scanning electron microscopy was conducted with a Hitachi S-900 FESEM (Hitachi Co, Lawrenceville, GA) scanning electron microscope. Samples were imaged at different magnifications using a 1.5 or 2 KV accelerating voltage.

3.3 Results:

The purpose of this study was to use encapsulated recombinant *E. coli* cells expressing AtzA to reduce atrazine in water. The gels have two desirable characteristics with respect to the herbicide; they are able to both adsorb atrazine and to transform it into hydroxyatrazine, which is dissimilar toxicologically from atrazine and is more biodegradable [40]. The cells were rendered non-viable to eliminate any risk of a potential release during use.

3.3.1 Encapsulated recombinant *E. coli* viability:

Different silica gel compositions were tested for encapsulation efficiency and enzymatic activity (Table 2.1). The ultrastructure of the gels showed uniform condensation and aggregation of silica nanoparticles (figure 3.1A) around the encapsulated cells, generating a hyperporous network. At lower resolutions (figure 3.1B) small groups of *E. coli* were observed to be homogeneously distributed across the volume of the gels. Figures 3.1C and 3.1D show the two geometries used in this study; microbeads and a cylinder block containing *E. coli* expressing AtzA, respectively. Cylinder blocks were used in initial experiments for optimization of the silica gel material and maximum bioactivity. In contrast, the microbeads were used for long-term activity assays and were developed for future field studies since they have the highest area:volume ratio and thus are expected to yield the highest activity (among offering other advantages).

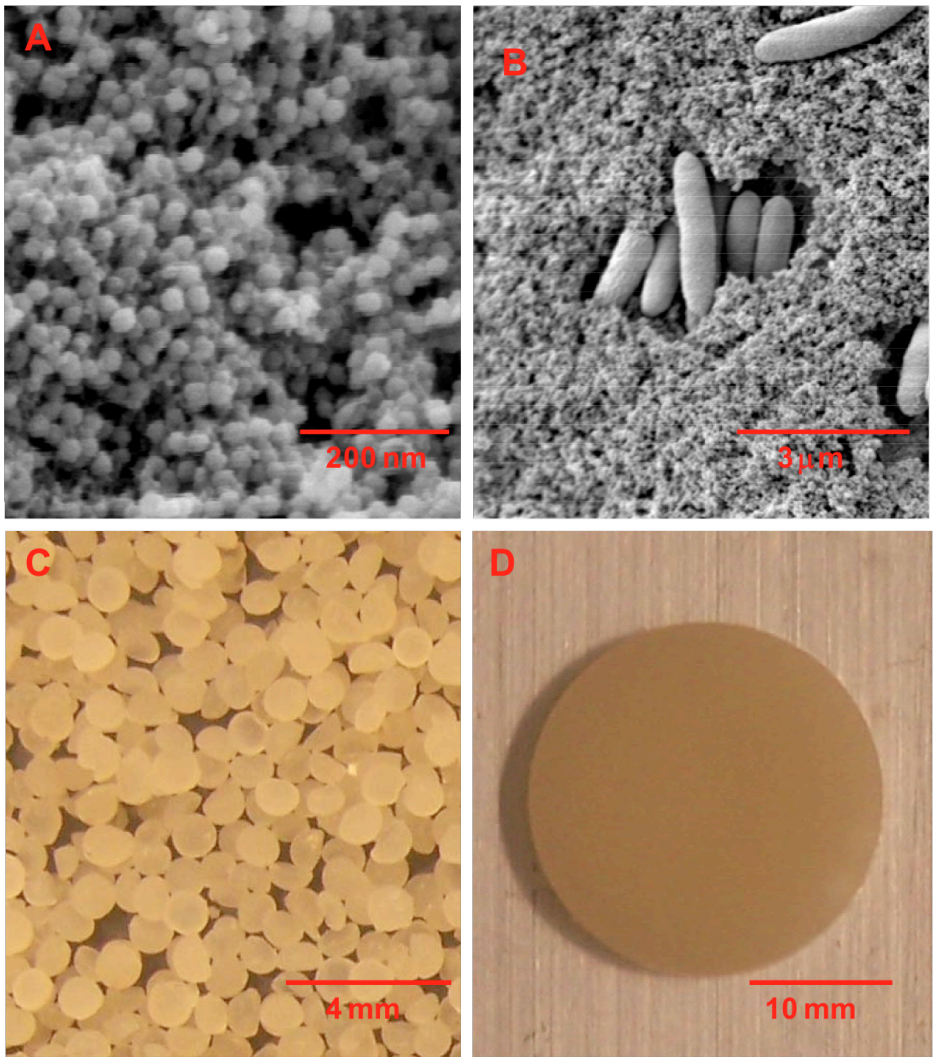

Fig 3.1: (A) Electron microscopy image showing the porous gel as aggregates of silica nanoparticles, (B) N1 gel containing *E. coli* cells expressing AtzA, (C) microbeads containing *E.coli* cells expressing AtzA, (D) cylinder block containing *E. coli* expressing AtzA.

Most of the studies conducted to date with encapsulated *E. coli* in silica gels focus on the long-term cell viability after encapsulation [41, 42]. However, the degradation of atrazine by recombinant *E. coli* expressing AtzA does not require viable cells since the atrazine is dechlorinated by a non-metabolic hydrolytic reaction [16]. This is a very important aspect for practical decontamination of drinking water since negligible (if possible, zero) viability of the encapsulated cells is required. This minimizes the environmental risks in case of an accidental release of the recombinant microorganisms. Therefore, we developed a way of minimizing the viability of the encapsulated cells.

Figure 3.2 shows the loss of viability of cells encapsulated in different porous gels as measured by colony forming units (CFU) per gram of gel material. When the N5 gels were incubated at 45°C for 24 h, a reduction in survival/viability of the encapsulated cells close to 99.9 % was accomplished. In fact, cell CFU counts were so low in the oven-treated N5 gels that they were below the detection limit of our assay; we could not physically plate enough gel material to obtain accurate cell counts. The cells extracted from the N1, N2, and N5 (non-thermally treated) gels after 3 weeks of encapsulation had 93.4 %, 49.3 %, and 92.2 % less viable cells, respectively, when compared to cells extracted at t = 0 weeks (Figure 3.2). This showed that encapsulation of *E. coli* in the gels non-thermally treated still contained viable cells even after a long period of time of encapsulation.

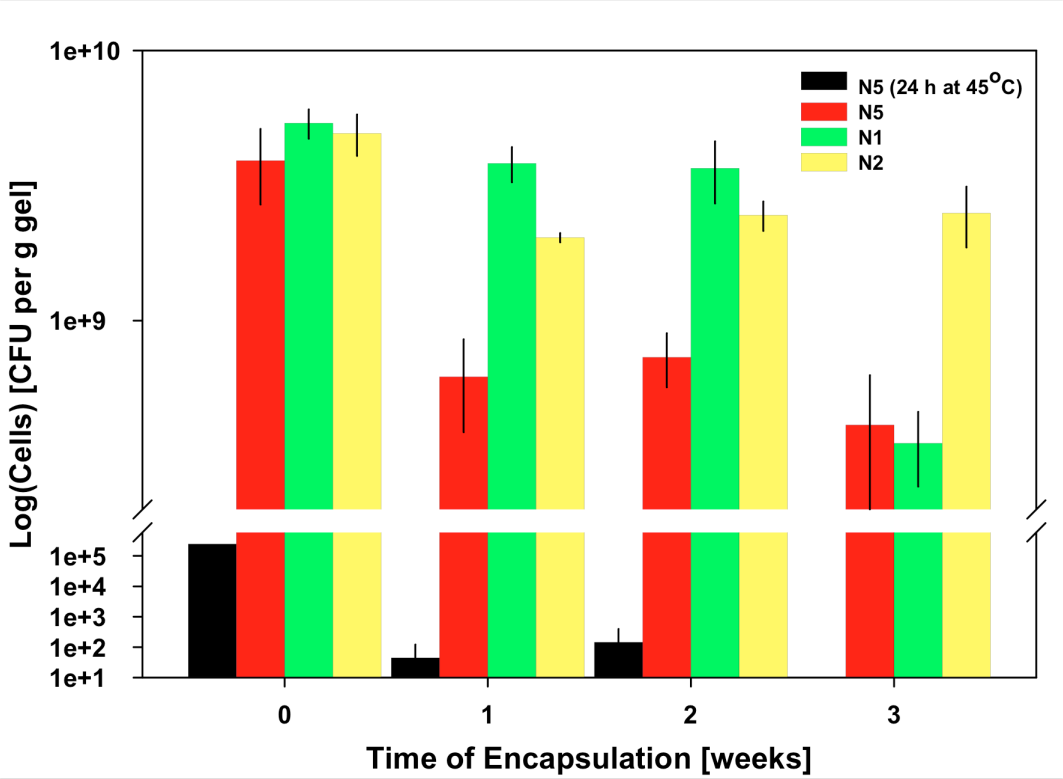

Fig 3.2: CFU of *E. coli* expressing AtzA extracted from different porous gels (n = 3). See Table 1 for gel composition.

3.3.2 Membrane analysis of encapsulated cells:

The reason for the significant decrease in survival of the encapsulated *E coli* with increased gelation temperature was explored using FTIR spectroscopy by monitoring the change in the location of the lipid acyl chain (ν-CH_2) stretching peak (located near 2850 cm^{-1} in solution). Before gelation, the ν-CH_2 peak locations of the cells in the silica solution were similar to the cells in water (Table 3.2) indicating that the micro-environment of the cells in the silica solution were similar to the cells in water. When the measurements were repeated 30 min after the gels were formed, the encapsulated cells had significantly lower ν-CH_2 values than the cells in water (Table 3.2). The decrease in the ν-CH_2 wavenumber reflects an increased packing of the membrane lipids of the cells due to encapsulation. When the encapsulated cells were incubated for 24 h at 45°C, there was a gradual shift in the ν-CH_2 peak location to higher wavenumbers, which indicated disruption of the cellular membranes of the encapsulated cells. In parallel experiments, encapsulated cells were dried over time at room temperature to monitor the changes in the ν-CH_2 peak position. The results showed that the ν-CH_2 peak position shifted towards higher wavenumbers as the sample was dried over time (Figure 3.3).

Temperature [°C]	ν-CH_2 Peak Position [cm^{-1}]		
	Solution	Gel	Gel (Thermally Treated)
4	2851.77 ± 0.1	2844.13 ± 0.2	2847.53 ± 0.6
10	2851.90 ± 0.0	2844.17 ± 0.1	2847.36 ± 0.8
23	2852.33 ± 0.1	2844.40 ± 0.2	2847.66 ± 0.8
37	2852.90 ± 0.0	2844.60 ± 0.1	2847.96 ± 0.1

Table 3.2: Changes in the structural conformation of lipid membranes of *E. coli* expressing AtzA with temperature and encapsulation conditions

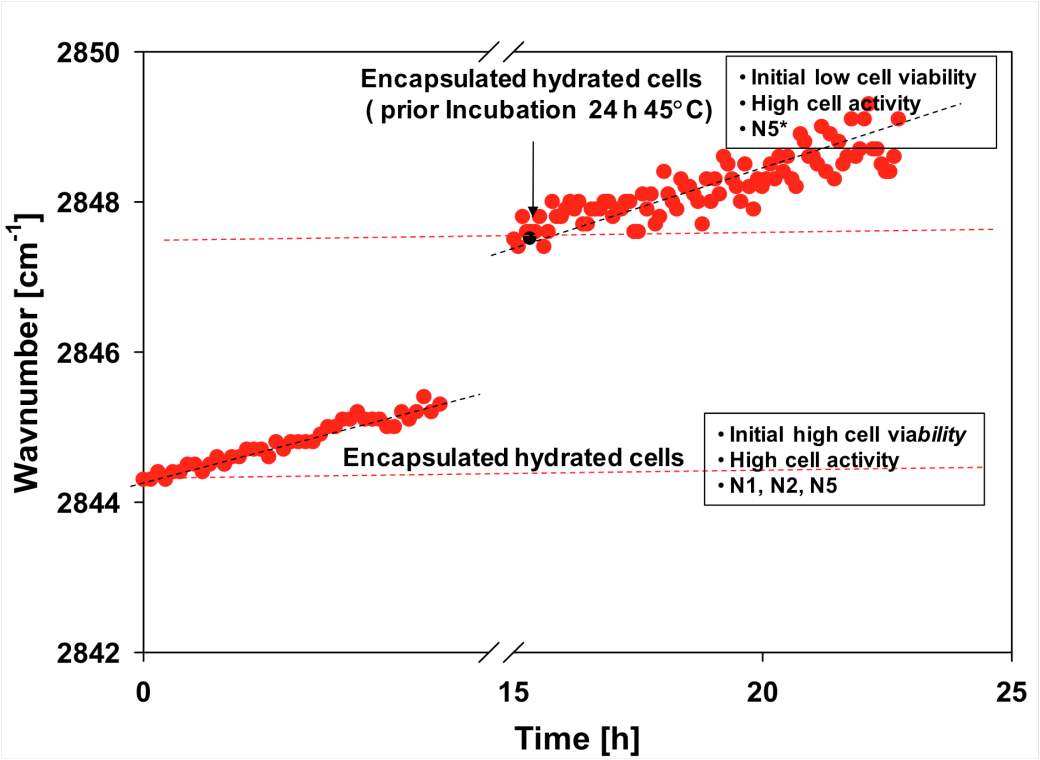

Fig 3.3: Time-dependent v-CH2 peak position of encapsulated *E. coli* expressing AtzA in silica gels

Additionally, measurements of the ν-CH_2 peak position for free and encapsulated cells at different temperatures revealed that the fluidity of the membrane decreased with encapsulation. For a temperature change from 4°C to 37°C, $\Delta\nu$-CH_2 was 1.13 cm^{-1} for the free cells while it decreased down to ~ 0.47 cm^{-1} for the encapsulated cells.

A comparison of the cells in solution and encapsulated cells did not show any significant difference in the morphology of their external membranes (Fig. 3.4A and Fig 3.4B). Distinctive raffles of the external membrane were observed in both cases. However, cells that were encapsulated and incubated for 24 h at 45°C did not have the same characteristics of the external membrane. Instead, the membrane looked shrunken and dehydrated (Fig. 3.4C). Both the FTIR analysis and SEM imaging showed the significant differences between the cells encapsulated at room temperature and the cells treated at 45°C which resulted in decrease viability (Table 3.2).

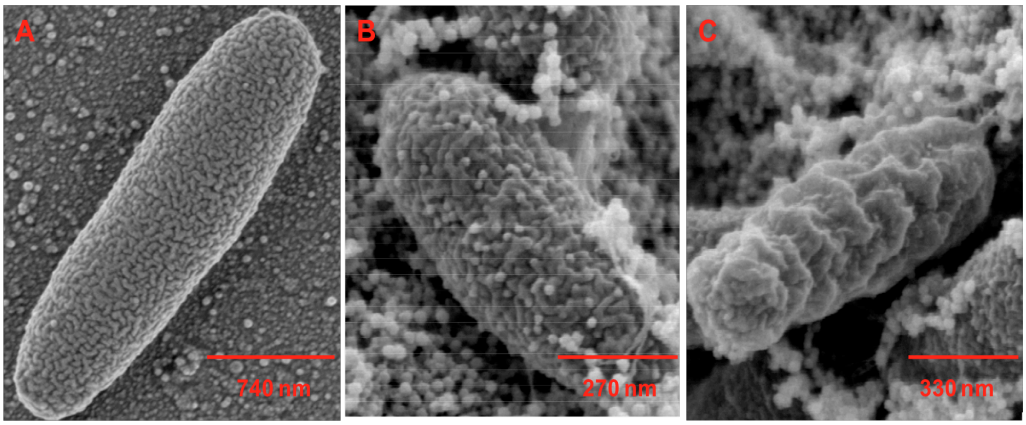

Fig 3.4: Electron microscopy images of *E. coli* expressing AtzA: (A) free cell in solution, (B) *E. coli* encapsulated in SPEG gel, N5, (C) *E. coli* encapsulated in SPEG gel, N5 after thermal treatment at 45°C.

3.3.3 Membrane permeabilization of *E.coli*:

Permeabilization was carried out as described in section 3.2.7. This study was carried out to select for the best candidate to permeabilize the cells without significant cell lysis and protein release. The permeabilization was required to analyze the effect of aging of encapsulated cells over a period of time. When, the cells were assayed over a period of time an increase in activity was observed over the first week, which was attributed to loosening up of the cell membrane thus allowing better diffusion of substrate into the cell. Flash frozen cells and untreated cells were used as controls for complete cell lysis and no lysis. It was observed that specific activity of cells increased to 3.7 times of normal cell activity with acetone and 4.6 times with triton X-100 (Figure 3.5). But, treatment with triton x-100 resulted in approximately 10 times more protein release (Figure 3.6). Hence, acetone was chosen as ideal candidate for permeabilization of cells for aging studies.

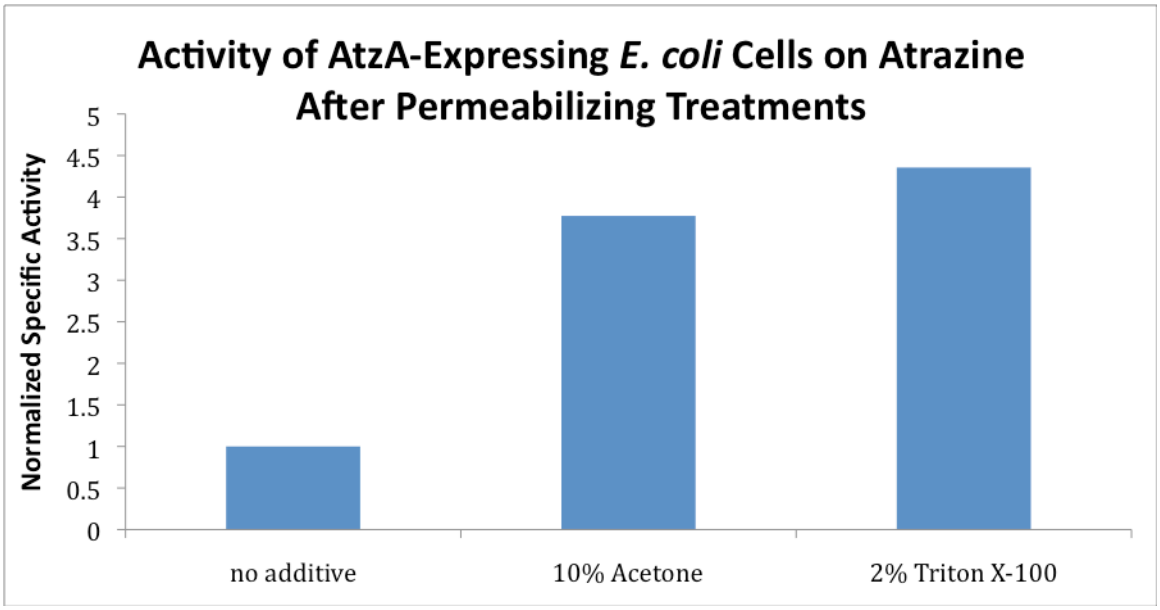

Fig. 3.5: Graph depicting comparison of normalized specific activity of permeabilized cells.

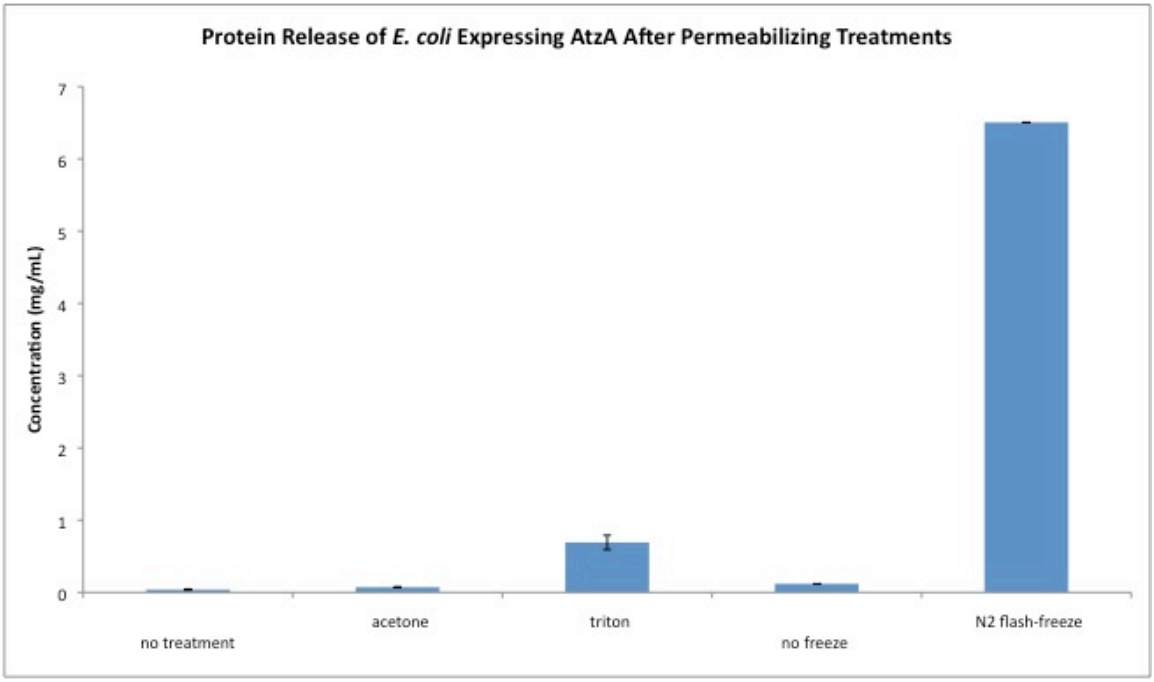

Fig 3.6. Graph depicting protein release because of permeabilization treatment. Flash freezing-thawing cycle and no treatment have been used as controls for complete lysis and no cell lysis respectively.

3.3.4 Effect of various additives on activity of *E. coli*:

The study was carried out to identify an additive for the silica matrix to increase its porosity along with stabilization of cells entrapped in the bead. Some, initial studies showed that diffusion of substrate into the beads was resulting in lowering of specific activity of cells inside the bead. Hence, the increase in porosity was desired for better diffusion of substrate into the bead and of product out of the bead. Polyethylene glycol, Trehalose and Pluronic F-127 were identified as most suitable candidates. The study was carried out as described in section 3.2.7. It was observed that presence of 10% PEG causes a 4 times increase in specific activity of the cells whereas presence of 20% trehalose results in 8 times higher cell specific activity (Figure 3.7). But, presence of trehalose at 20% concentration was resulting in higher amount of cell lysis as indicated by the decrease in OD_{600} value of the solution (Figure 3.8). Hence, 10% PEG was chosen as the ideal candidate for the matrix.

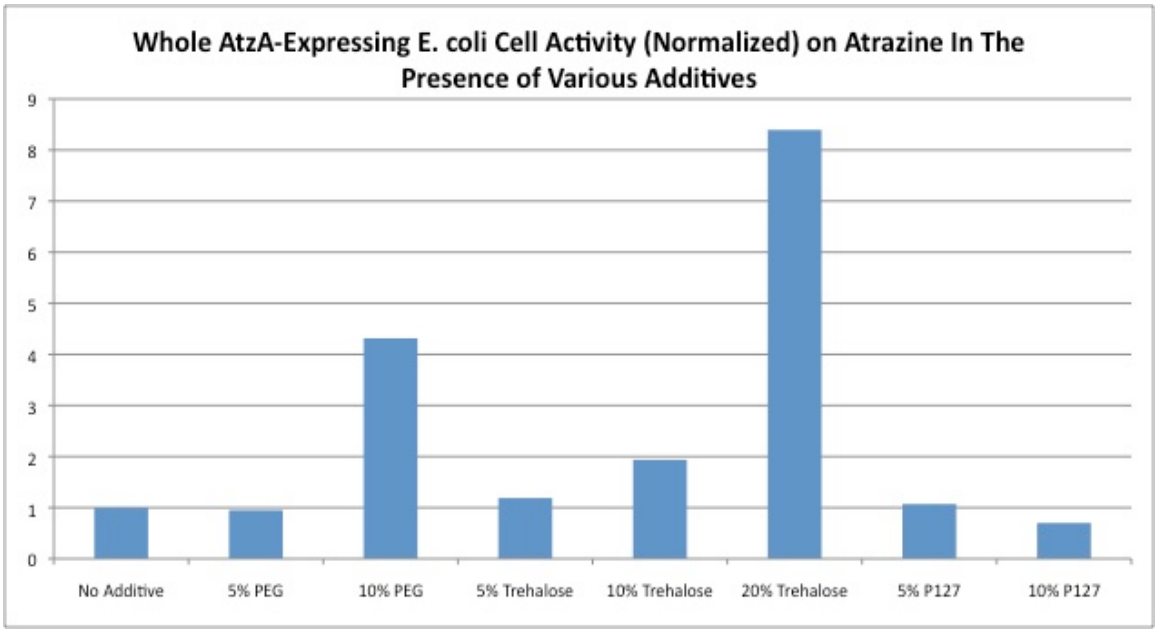

Fig. 3.7: Graph depicting comparison of normalized specific activity of cells incubated with different concentrations of additives.

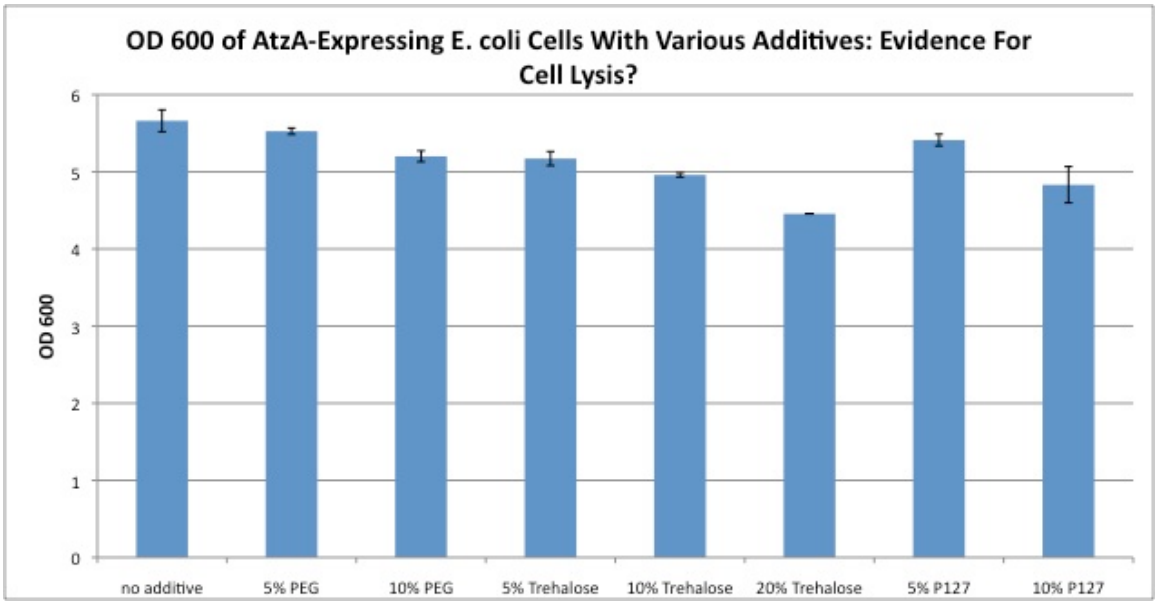

Fig. 3.8: Graph depicting normalized OD_{600} values of cell samples incubated with different concentrations of additives to check for cell lysis.

2.3.5 Atrazine biodegradation:

Atrazine degradation activity of the encapsulated microorganisms was evaluated using HPLC analysis. Due to the high atrazine adsorption characteristic of the gels, the rate of hydroxyatrazine production was used in all activity calculations.

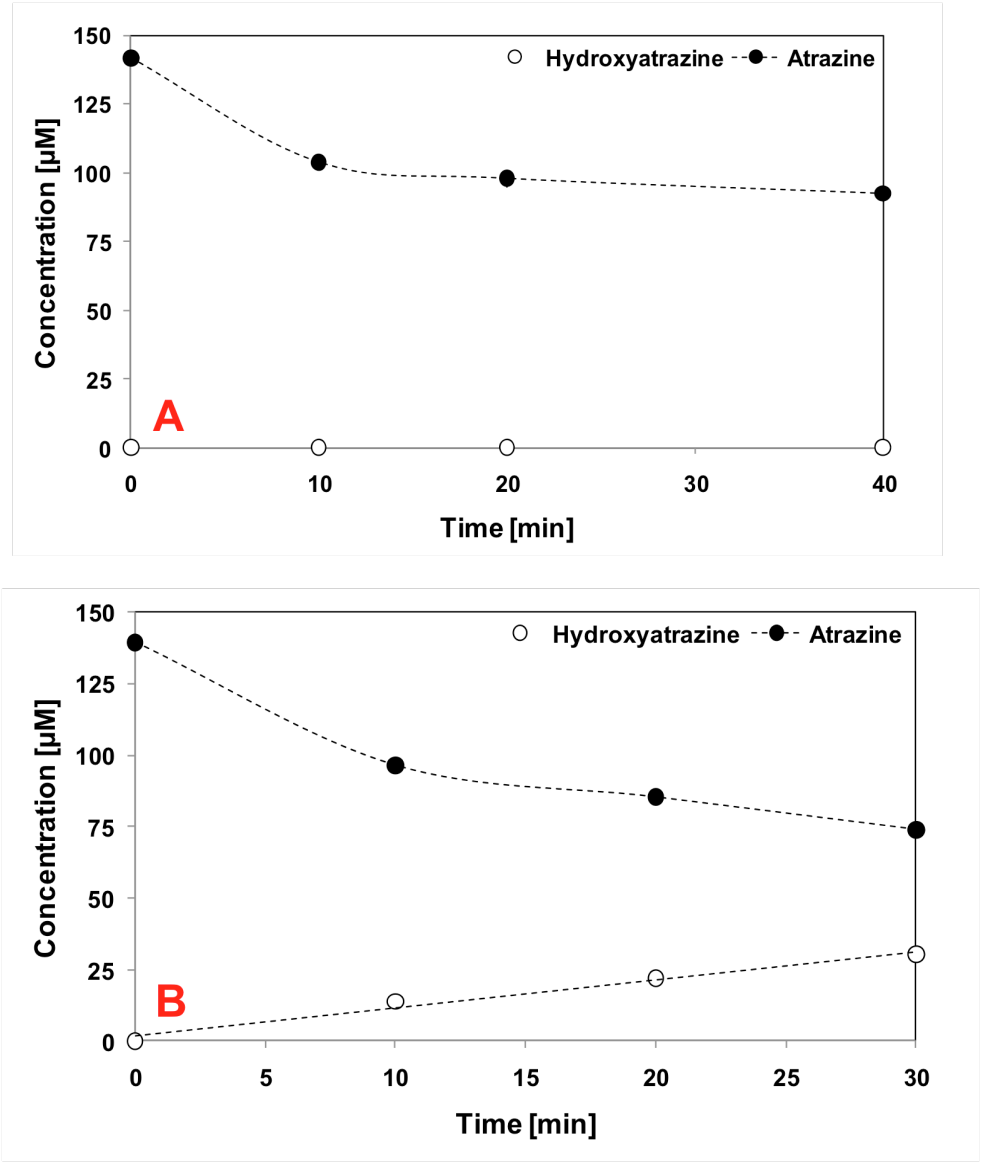

Fig. 3.9: Changes in atrazine and hydroxyatrazine concentration in solution: (A) adsorption of atrazine, (B) adsorption and biodegradation of atrazine (n = 3). The error bars are smaller than the symbols.

Figure 3.9A illustrates the atrazine adsorption ability of the gels by showing the change in atrazine concentration when exposed to silica beads that do not contain any cells. In the first 10 minutes, there was almost a 30 % decrease in atrazine concentration in the solution. As expected, hydroxyatrazine was not detected in this solution due to the absence of the enzyme AtzA. Figure 3.9B shows the drop in atrazine concentration via the combined effect of atrazine adsorption by the silica gel and the degradation of the atrazine by the encapsulated cells. The rate of hydroxyatrazine production was linear over time, which indicated that hydroxyatrazine had less affinity to the silica gel and was more readily released into the solution environment. This observation was supported by assays similar to those shown in Figure 3.9A but with hydroxyatrazine and cell-free beads (Figure 3.10).

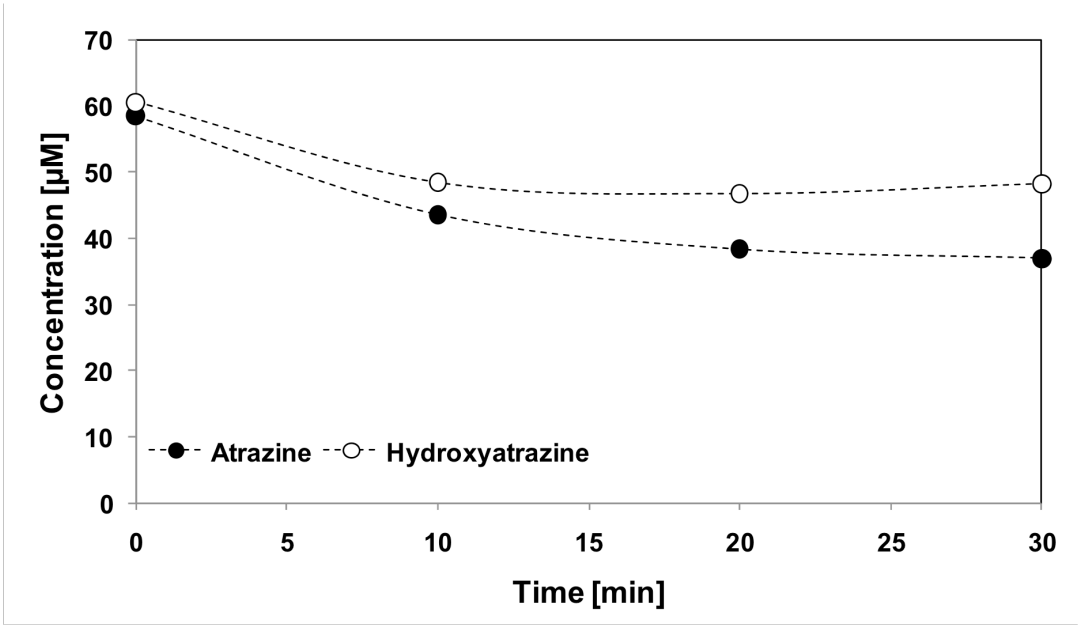

Fig. 3.10: Adsorption of atrazine and hydroxyatrazine in cell-free microbeads

Table 3.3 summarizes the results of the atrazine conversion activities obtained using different gel compositions and geometries (cylinder block vs. microspheres). The activity in cylinder blocks was significantly lower than those encapsulated in microbeads. This result was expected since only one surface of the cylinder was exposed to the solution, requiring the extensive diffusion of atrazine and hydroxyatrazine into and out of the gel, respectively. Cells encapsulated in N1 and N2 gels in cylinder blocks had only 16 %, and 22 % of the activity of the free cells in solution. As expected, gels that contained cells that did not express AtzA (N3) or gels that did not contain any cells (N4) did not show any hydroxyatrazine production. It was not possible to test the N1 and N2 gels in microbead form since the microbeads did not show any mechanical integrity and got easily pulverized. This made them unsuitable for any bioremediation application in the field. On the other hand, the N5 gels could easily be manufactured in the form of cylinder blocks and microbeads. Note the significant increase in specific activity when the cells were encapsulated in the high specific surface area microbeads (N5*) when compared to the gels encapsulated in a cylinder block of limited specific surface area (N5).

Table 3.3: Comparison of normalized activity of encapsulated and free *E. coli* expressing AtzA in different gels. Note that (*) indicates microbeads. Rests of the gels were tested in cylinder form. N3 gels contained non-expressing cells, N4 gels did not contain cells. Activity was measured at room temperature after 24 h of encapsulation

Normalized Specific Activity [μmol/min.g]	
Gel Type	**Hydroxyatrazine**
N1	0.159
N2	0.224
N3[a]	0.000
N4[b]	0.000
N5	0.124
N5*	0.953* ± 0.35
Free Cells	1.000

[a] gels containing non-expressing cells

[b] gels containing no cells

* microbead form

Note: The activity of all the gels was normalized by dividing observed specific activity of gels with free cell activity of the cells used for encapsulation. This was done to take into account the variation in activity between different batches of cells.

Figure 3.11 shows the activities of the free and microbead encapsulated cells (N5*) over 4 months. When the activity was measured at room temperature, free cells showed an average of 0.61 ± 0.04 μmol/g-min of activity over 21 days. After 21 days, significant cell lysis was observed in the free cells; this was likely due to long-term hypo-osmotic stress induced by water. Therefore, the experiments on the free cells were stopped at that time point. On the other hand, cells encapsulated in N5 porous gels (microbeads) showed a stable activity between 0.44 ± 0.06 μmol/g-min to 0.66 ± 0.12 μmol/g-min for up to 4 months. This showed that even though the encapsulated cells were non-viable and had lost some membrane integrity, AtzA was protected and active in the silica matrix. The activities of the free and encapsulated cells were found to be temperature dependent. At 4°C, activity dropped by 45 % and 30 % for the free and encapsulated cells, respectively. The activity of encapsulated cells at 4°C was 33.3 % higher than the cells in solution.

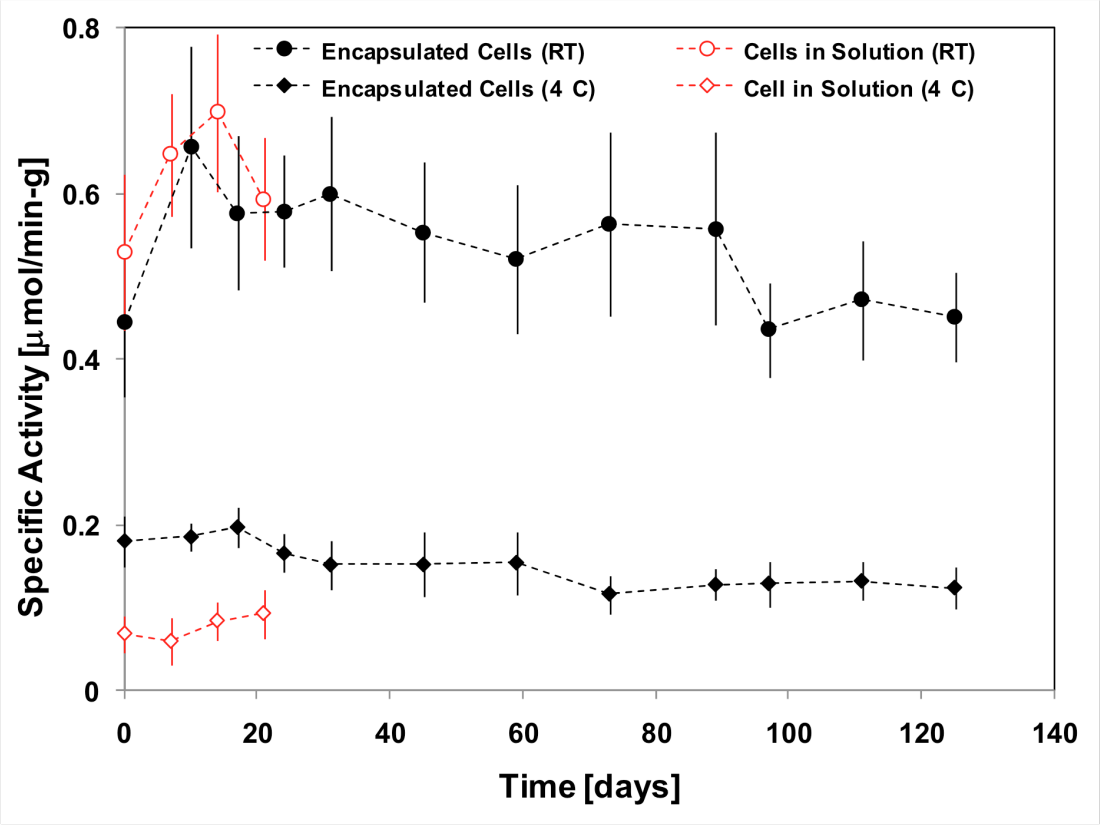

Fig. 3.11: Specific activity of the non-viable *E. coli* expressing AtzA in N5* porous microbeads at different temperatures (n = 4).

For activity measurements at room temperature, at 10 days of encapsulation (~ 7 days for free cells), there was an improvement in the activity, which was attributed to an increase in the permeability of the encapsulated cellular membranes since the viability of the encapsulated cells (N5, 24 h at 45°C) becomes even more negligible (Figure 3.12). This is further supported by parallel experiments with acetone as a permeabilizing agent, where cells showed higher activities when compared to free and encapsulated cells (Figure 3.12).

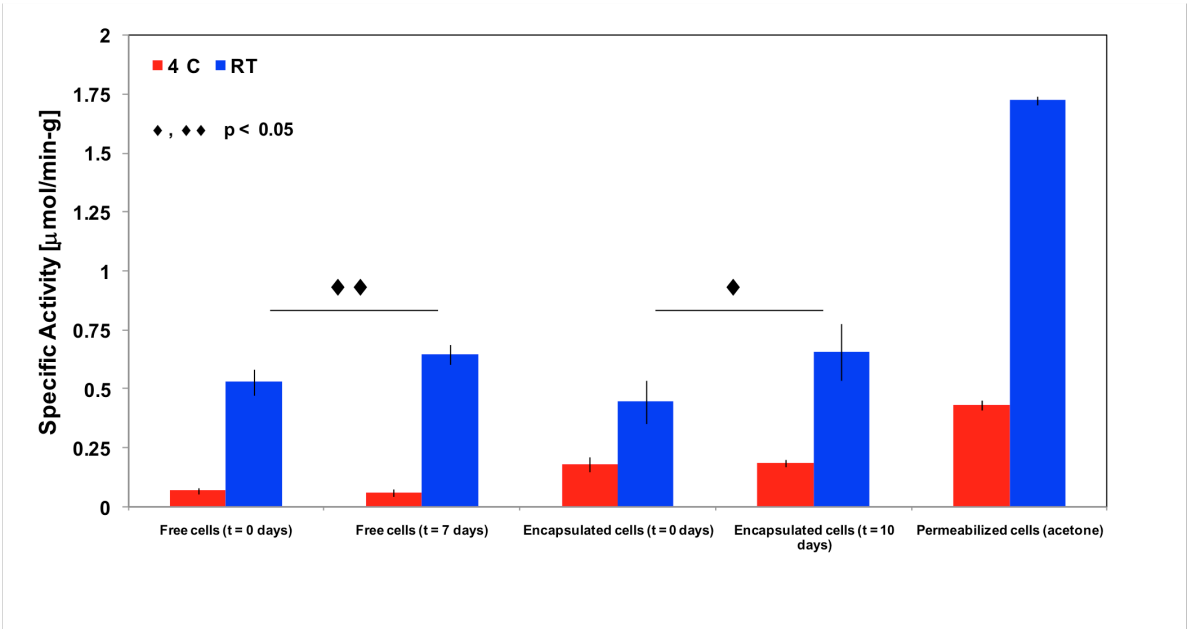

Fig. 3.12: Comparison of specific activity of *E. coli* expressing AtzA at different conditions

However, for activity measurements at 4°C, the improvement was only significant for cells in acetone; which indicated that the activity of the enzyme not only depended on the permeability of the membrane but also on the temperature at which the assays were carried out.

3.4 Discussion

Activated carbon is widely used for removing contaminants in public drinking systems. However, activated carbon particles do not have selective adsorption for chemical compounds and also adsorb naturally occurring organic compounds, which compete with atrazine for adsorption on charcoal causing displacement of the adsorbed atrazine. Studies show that the presence of natural organic matter in the water reduces the adsorption kinetics of activated carbon and its capacity of atrazine adsorption [43, 44]. The optimal operation conditions of the charcoal can thus get affected by this atrazine displacement and result in desorption of trace organic pollutants into the environment. Therefore, there has been a search for alternative technologies that have high adsorption potential and selectivity. So far, the use of organoclays [45], chemically modified carbon [46], dialysis [47], UV light photodegradation [48], nanofiltration [49], non-ionic polymeric resins [50], covalent sequestration [44], and ozone and OH radicals [51] has been examined. Even though these technologies have proven to be effective at the laboratory scale, but their widespread implementation has been limited by their efficiency and cost in comparison to activated carbon. In this study, an economical hybrid biomaterial was developed that possesses the adsorptive capability of activated carbon but in addition, selectively degrades atrazine. Moreover, the combination maintains atrazine removal capabilities for extended periods without saturation, thus eliminating the need for recharging.

3.4.1 Viability of the encapsulated cells:

Many intracellular microbial enzymes are produced in quantities large enough to be used in industrial processes. However, the cost for their isolation and purification can be quite high. Hence, direct encapsulation of whole cells such as yeast or bacteria it has been of widespread interest in order to avoid tedious separation and purification procedures. Dead bacteria cells can behave as a ‘bag of enzymes’ and retain enzymes within their natural surrounding in turn, preserving their stability and avoiding leaching during repetitive operations. Many bacteria have been immobilized in silica-based porous gels with the aim of developing biosensors, bioreactors, or bioremediation applications that

require metabolically driven reactions [52, 53]. All of these applications require long-term cell viability after the encapsulation process. This requirement has directed most research towards improvement of the survivability of the cells in the silica gels by using milder encapsulation methods [54], or by the addition of osmoprotectants [41, 42]. On the other hand, reactions that do not require metabolic activity, such as the hydrolytic removal of chlorine from atrazine, do not necessitate such considerations. It has been shown that recombinant *E. coli* cells expressing AtzA can still be highly active enzymatically without being viable [16]. In fact, for a drinking water application, non-viable encapsulated bacteria are desirable to mitigate against human exposure to bacteria, despite the known safety of the bacterial species used in our studies.

E. coli cells survived the process of encapsulation in the different gels tested when not cured at a high temperature (Figure 3.2). Clusters of cells were distributed evenly through the gel. The porosity of the gel was in the nanometer range, which restricted the cells from migrating, growing and undergoing cellular division. The gels were permeable to water and to water soluble solutes (including atrazine and hydroxyatrazine) and gases. The viability of encapsulated cells changed depending on the composition of the gels. Within 3 weeks, there was a 93.4 % reduction in viable cells encapsulated in N1. It has been shown that surface silanol groups of the silica gels have a detrimental effect on the integrity of the cellular membranes of the encapsulated cells. This is thought to be one of the main reasons for the decrease in viability and survival of the encapsulated cells along with the lack of space for cellular division [41, 55].

The formulations N1 and N5 had the greatest decrease in viable cells after 3 weeks, 93.4 % and 92.2 %, respectively. In contrast, N3 gels had the highest viability after 3 weeks of encapsulation, with only a 49.3 % decrease. This result was consistent with reported values of viability of encapsulated *E. coli* TG1/pPBG11 cells using alkoxides and PEG as precursors of the porous gel [54]. However, 6.6 % or 7.8 % viability of encapsulated cells after 3 weeks was still too high for using bacteria in the purification of water.

The number of viable cells after encapsulation was highly reduced with a thermal treatment step where the encapsulated cells were incubated in a convection oven for 24 hours at 45°C. This treatment resulted in a viability decrease of almost 100 % based on CFU counts. We suggest that this drop in viability is the result of a loss of cell membrane integrity. This hypothesis is supported by the structural changes observed via FTIR analysis in the lipid membranes of encapsulated cells due to thermal treatment. After encapsulation, there was a drop in the ν-CH_2 peak position, which indicated an increase in the packing of the membrane lipids. This could be due to specific bonding between the silica surface silanol groups and the lipid headgroups and/or dehydration due to extensive hydrogen bonding of the silica gel, and shrinkage. However, the initial decrease in the lipid headgroup spacing did not have a significant effect on the viability of the encapsulated cells since cells extracted from the gels after a short period of time could continue to grow and form colonies. On the other hand, when the encapsulated cells were thermally treated, ν-CH_2 peak position further shifted from ~ 2844 cm^{-1} to ~ 2847 cm^{-1} in an irreversible fashion, which indicated a permanent disruption of the lipid membrane. Comparisons of electron microscopy images of cells in solution and extracted cells from gels with and without thermal treatment showed the significant difference in the texture of the lipid cell membranes.

3.4.2 Atrazine biodegradation:

Pseudomonas sp. strain ADP and purified AtzA have previously been encapsulated in silica gels for the purpose of biodegradation of atrazine [34, 56]. When a combination of alkoxide precursors is used for the synthesis of the silica gel, the encapsulated AtzA remained active for up to 3 weeks while maintaining 40 % of the activity of the free AtzA [56]. In contrast, it was reported that the encapsulated *Pseudomonas* sp. strain ADP required viability to biodegrade up to 60 % of the atrazine present in solution. Otherwise only 8 % atrazine biodegradation occurred [34]. In addition to the low performance detailed above, the further disadvantages of these two approaches are that AtzA requires an extensive process of purification, cells need to be alive and

supplemented with nutrients, and the encapsulation process must not yield to detrimental by-products such as methanol that can seriously reduce the activity of the enzyme or the viability of the cells. The encapsulation of recombinant *E. coli* cells expressing AtzA in silica or SPEG gels overcame all the previous limitations, since the encapsulated cells did not require viability in order to maintain activity of AtzA. The hybrid biomaterial we have developed not only mimics the adsorptive capabilities of activated carbon, but also provides an avenue for in situ herbicide degradation.

The adsorption of atrazine by silica was evident when gels that did not contain cells were incubated in the presence of 140 μM atrazine (30.2 ppm); there was a drop in the concentration of atrazine with two characteristic slope regions (Fig. 3.9A). We suggest that the initial steeper slope indicated atrazine adsorption on the surface area within the silica matrix. As available atrazine binding sites decreased, atrazine adsorption slowed as indicated by the second slope. When cells were present in the porous gel, the slopes observed were steeper (i.e., more rapid depletion of atrazine) along with the production of hydroxyatrazine was indicative of the atrazine adsorption and biodegradation working in tandem. This combined mechanism of action was corroborated by the generation of hydroxyatrazine in the solutions exposed to gels with encapsulated cells (Fig. 3.9B).

All specific activity calculations were based on the rate of hydroxyatrazine production to avoid overestimation of the values of atrazine biodegradation; hydroxyatrazine adsorption in the porous gel was lower than what is seen with atrazine (Fig. 3.10). The specific activity of the enzyme after encapsulation of the cells depended on the precursors used for the gel synthesis and on the geometry of the gel (e.g., cylinder block or microbeads). In cylinder blocks, the activity ranged from 15 % to 22 % of the cells in solution. The low surface area per volume ratio limited the diffusion of atrazine and hydroxyatrazine through the cylinder block gel and was responsible for the low specific activity. It is known that the rates of diffusion in silica gels are slow [57]. One possible solution to this problem would be to increase the porosity of the silica or SPEG

gels, but this was not done to ensure that the encapsulated cells remained entrapped in the gel matrix. Instead, microbeads with a diameter of ~ 1 mm with significantly higher specific surface area, but similar porosity as cylinder blocks were manufactured.

The activity of the encapsulated cells in microbeads ranged between 0.44 ± 0.06 μmol/g-min to 0.66 ± 0.12 μmol/g-min. This activity was comparable to free cells (Fig. 3.12). However, free cells lysed after 21 days, and were not suitable for further activity assays. In contrast, encapsulated cells in microbeads had stable activity for up 4 months. We suggest that although encapsulated cells are not viable and have disrupted lipid membranes after thermal treatment (Table 3.2 and Fig. 3.4C), most of the AtzA enzyme was still active and distributed in what remained of the encapsulated cells, or was adsorbed to the surface of the porous gel.

As expected at 4°C, there was a drop in the specific activity of both encapsulated and free cells. It is known that structural changes of enzymes in solution and in crowded environments (e.g., cytoplasm of a cell) are temperature dependent (Eisenthal et al., 2006, Reátegui and Aksan, 2010). Moreover, the lipid membrane of the free cells transitioned to a more ordered state at 4°C (lower ν-CH_2 peak position). This was not the case for the membranes of encapsulated cells that had undergone the thermal treatment (Fig. 3.4C). We believe that in free cells at 4°C, the membrane becomes a strong barrier to the diffusion of atrazine into the interior of the cell due to its more ordered, tightly packed configuration. In heat-treated encapsulated cells at 4°C, the cell membrane is perturbed and therefore unable to transition into the ordered state seen in the normal membrane; it is less of a barrier to atrazine diffusion and therefore we observe a higher specific activity for encapsulated cells at 4°C.

3.4.3 Mathematical model to analyze effectiveness of immobilization system

Hence, here we are trying to analyze the kinetics of the cells in silica beads in our system to estimate the effectiveness of the immobilization system. The system was analyzed on the basis of normalized specific activity by carrying out parallel experiments with free cells in solution. But, as entrapped catalyst systems are very different from soluble catalyst in solution. In these systems for substrate to come into contact with the catalyst it needs to diffuse through the particle (silica bead in our case). In most of the cases the diffusion coefficient for this is different from the bulk diffusion coefficient and is called the effective diffusivity of the substrate in the particle matrix and is given by the equation:

$$D_{eff} = D\,(\varepsilon/\tau)H \quad .....(1)$$

Where, D is the bulk diffusivity

ε is the porosity of the bead

τ is the tortuosity factor (assumed to be in range 1.4 to 7)

H is the hindrance factor, which can be excluded if radius of pore is much larger than radius of substrate molecule

To analyze the system for mass transfer effects the model previously described [58] was used, as the assumptions stated for the model were reasonably true for our present system and are listed below:

1. The silica bead has an uncharged matrix.
2. The *E.coli* cells are distributed uniformly throughout the particle.
3. Transport of atrazine through the silica bead follows Fick's law and the effective diffusivity of atrazine remains constant throughout the reaction.
4. The reaction is isothermal and there is no change in pH.
5. All electrostatic effects are negligible.
6. The concentration of substrate is at the external surface of a bead is equivalent to that in the bulk.

The general differential equation for mass transfer in an immobilized catalyst bead is given by

$$\frac{\partial S_i}{\partial t} = \overline{\nabla N_s} = v(S_i)$$

Where, $\overline{\nabla N_s}$ is the net molar efflux rate of the substrate. Considering our system is a spherical system of bead radius R. At steady state, $\frac{\partial S}{\partial t} = 0$, and if we assume that diffusion occurs only in the radial direction, the steady state material balance becomes

$$\frac{d^2x}{d\bar{r}^2} + \frac{2}{\bar{r}}\frac{dx}{d\bar{r}} = \frac{R^2 v(S_i)}{D_{eff} S_0} = \frac{R^2 (v_{\max} / K_m D_{eff}) x}{1 + \beta x}$$

Where, dimensionless internal concentration $x = \frac{S_i}{S_0}$,

dimensionless radial coordinate $\bar{r} = r / R$,

dimensionless bulk concentration $\beta = S_i / K_m$

From the above equation it can be observed that the concentration profile in the silica bead will depend on the size of the bead, the effective diffusivity of atrazine through the bead and the intrinsic kinetic parameters of the immobilized enzyme. All these factors are combined in a single dimensionless parameter called the *Thiele modulus* Φ, defined for Michaelis–Menten kinetics by

$$\phi = \frac{R}{3}\left(\frac{v_{\max}}{K_m D_{eff}}\right)^{1/2} \qquad \text{.....(2)}$$

The physical significance of this is that the square of *Thiele modulus* is the ratio of an intrinsic reaction rate in the absence of mass transfer limitations to the rate of diffusion through the particle and can be related to an effectiveness factor η defined for coupled intrabead diffusion-reaction. However, calculation of thiele modulus requires knowledge of intrinsic rate parameters, which cannot be obtained directly from diffusion affected reaction rates. To overcome this an observable modulus is defined for a sphere as

$$\mathbf{\Phi} = \frac{v_{obs}}{D_{eff} S_0}\left(\frac{R}{3}\right)^2 \qquad \text{.....(3)}$$

η= observed reaction rate/rate in the absence of intrabead conc. gradients.

The factor can be determined if the observable modulus value and the value of β is known by using the chart in figure 3.13 [58].

Hence, to estimate the effectiveness factor of our system we need to calculate the effective diffusivity. D_{eff} is calculated using equation (1). We can ignore the hindrance factor H because diameter of atrazine molecule is about 9 Å [59] and from electron microscopy experiments the diameter of a pore in the bead is estimated to be 25 nm. Hence, the size of molecule is much smaller than that of the pore. Therefore,

$$D_{eff} = D\ (\varepsilon/\tau)$$

For atrazine D= 5.57 x 10^{-6} cm^2/sec [60]

Assuming, tortuosity τ to be average of the lowermost and highest value = 4.2

Estimated Porosity $\varepsilon = 1-(\rho_{bulk}/\rho_{particle}) = 1-(1.25/2.65)=0.53$,

where, the value of ρ_{bulk} has been calculated on the basis of mass and size measurements for beads and $\rho_{particle}$ is assumed to be the value of density of silica.

Hence, D_{eff}= 0.7 x 10^{-6} cm^2/sec

Substrate conc. S_0 = 150 µmol/L

Radius of beads R = 1000 µm

Density of beads = 1.25 g/cm^3

Cell loading = 0.08 g/g of matrix

From gel densitometry data we know only 10% of total cell protein is AtzA.

Enzyme loading = 2.613 x 10^{-3} µmol enzyme/g of matrix

Measured reaction rate = 252 µmol of atrazine/µmol enzyme

Hence, by plugging the values in (3) we get,

$$\Phi = 4.35$$

Value of intrinsic K_m is assumed to be equal to that of the free enzyme i.e. 149 µM [28].

$$\beta = S_0/K_m \cong 1.0$$

Hence, from literature looking at corresponding values of effectiveness factor for the calculated value of the modulus we get, $\eta \approx 0.38$.

From this model it is observed that even though we get specific activity value for microbeads to be 95 percent of the free cells in solution, the effectiveness factor of the system depending on the mass transfer limitation due to material properties is 0.38. This difference can be due to the effect of the immobilization process and effect of various components of the silica matrix such as PEG which is not taken into account during estimation of free cell activities. As, it has been shown from separate experiments that permeabilization and incubation with PEG results in cells with higher specific activity. The porosity of the matrix could not be increased for improved effectiveness to ensure that the encapsulated cells remained entrapped in the gel matrix.

3.4.4 Mathematical model to analyze the atrazine removal rate of the system

The biocatalyst developed in the study results in removal of atrazine due to two separate mechanisms working in parallel. When we carried out kinetic analysis with data from atrazine disappearance and hydroxyatrazine appearance, a difference in observed specific activity values was seen. Following experiment with cell free beads showed decrease in atrazine concentration with time. The slope of disappearance decreases as equilibrium concentration of atrazine is approached. This effect of atrazine adsorption to silica has been widely studied and is shown to follow the Freundlich isotherm [61].

$$\tau = K_F C_{eq}^{n}$$

where, Γ (μg/m2) is the surface concentration of atrazine, K_F ($\mu g/m^2$)($\mu g/ml$)$^{-n}$ is the Freundlich coefficient, which shows the affinity of sorbate with sorbent, C_{eq} (mg/L) is the equilibrium concentration of atrazine in electrolyte solution, and n (dimensionless) is the Freundlich exponent. The values of these corresponding to systems close to our reaction system from the literature are K_F=0.0142 and n=0.936 [61,62].

The net rate of atrazine disappearance can be represented by the following equation:

Rate of atrazine disappearance = Rate of adsorption + Rate of biodegradation

This can be represented as

$$v_{net} = v_{abs} + v_{\deg}$$

Kovaios et al. (2011) have shown in their work that in aqueous solutions atrazine adsorption to silica follows Elovich's kinetic equation. Using their model we get

$$\frac{dS}{dt} = \alpha e^{-\beta S} + \frac{V_{\max} S}{K_m + S}$$

Values of constants α and β can be found from the literature [62]. But, for K_m as it is an intrinsic parameter of the system, could not be determined.

As both terms in the above equation for the known values of constants will be positive the equation supports our hypothesis that the system allows for faster removal of atrazine than the specific activity rates reported here. As, the specific activity values reported are just based on hydroxyatrazine disappearance. This hypothesis is further supported by the experimental data presented in figure 3.9B. It can be seen that slope for initial rate of atrazine disappearance is higher than that of appearance of hydroxyatrazine. This localization of atrazine on the bead is important as the biocatalyst has been developed keeping the existing flow through water treatment systems in mind and can affect the flow rates of water that maybe used for degradation of atrazine to concentrations below the desired limit.

In summary, we developed an effective approach for the bioremediation of atrazine in water. The method consisted of the encapsulation of recombinant *E. coli* expressing AtzA in porous silica gels. The synergistic interaction between the porous silica and the cells allowed the adsorption and biodegradation of the atrazine for over 4 months. The rates of conversion of atrazine by the encapsulated cells depended on the precursors used for the synthesis of the porous gels and on their final geometries (e.g., films or microbeads). When

microbeads were used the rates of biodegradation of atrazine were close to the values obtained with free cells.

Chapter 4: Conclusions

4.1 Mutant atrazine chlorohydrolase characterization:

We were able to design an effective expression vector and production protocol for the protein. High yields of soluble protein were observed when the gene was cloned in the vector and expressed in *E. coli* bacteria. Also, an efficient purification protocol was developed to provide high yields of up to 15 mg of purified protein per liter of bacterial culture using his-tag affinity chromatography. Preliminary studies were successfully carried out for comparison of characteristics of the mutant enzyme to the wild type enzyme. These studies provided valuable insight into future studies required to gain more knowledge about the effectiveness of the mutations carried out in the active site of the protein. The observed K_{cat} value for the mutant enzyme differed significantly from the published value and was very close to the K_{cat} value of the wild type enzyme. Further, the second hypothesis for the decrease in size of the mutant enzyme isopropyl binding site did not hold true on preliminary testing with bigger butyl side chains. Though further studies are required for complete characterization of the mutant strain. For the scope of this project the mutant enzyme was not found to be more efficient then the wild type enzyme which was the goal of this study.

4.2 Silica gel encapsulation system for atrazine degrading *E. coli*:

Also, an effective immobilization system was developed for biodegradation of atrazine in water filtration systems. The system consists of immobilized atrazine chlorohydrolase expressing bacterial cells in a silica-PEG matrix. The immobilized enzyme was found to be active for a period of over 4 months and showed higher activity and stability at lower temperatures inside the matrix as compared to free enzyme in solution. The effectiveness factor η, for the system obtained from mathematical modeling was observed to be 0.38. The immobilization process was modified to make sure that the number of viable cells inside the matrix was close to zero to ensure complete safety of the product for practical applications and to take care of any regulatory concerns. Even though the bacterial strain used is a proven non-pathogenic strain. The cell viability was confirmed by plating crushed silica beads on agar plates and incubating them at 37 °C for 48 hours.

4.3 Future Directions:

- A directed study involving comparison of substrate specificity of triazine ring substrates having bigger side groups then atrazine with both mutant and wild type atrazine chlorohydrolase. The study will be highly insightful in understanding the effects of mutations carried out in the active site of the enzyme.
- Further studies are required to determine the effect of the His-tag on the structure and activity of mutant AtzA. A good approach would be to compare the activity of the mutant enzyme in the same vector as the wild–type enzyme without the his-tag. This will prove to be the final piece required to compare the specific activities of the mutant and the wild type under similar reaction and expression conditions.
- A study needs to be carried out directed at finding the optimum storage conditions for the beads, which are cost effective and also maintain the activity and stability of the product.
- Studies need to be carried out at low concentrations (4-5 ppb) of atrazine to test the product at actual environmental concentrations.
- Field-testing of the biocatalyst in a flow through water treatment system needs to be carried out to get more information about the performance of beads, which will be helpful in their optimization.
- Cocktail of biocatalysts can be developed for removal of multiple compounds from wastewater by using a mixture of beads containing different bacteria or beads containing a mixture of bacteria.

References:

1. Radosevich, M, Traina, SJ, Hao, Y-L & O.H.Tuovinen (1995) Degradation and mineralization of atrazine by a soil bacterial isolate. Appl Environ Microbiol, 61, 297 - 302.
2. Macias-Flores, A, Tafoya-Garnica, A, Ruiz-Ordaz, N, Salmeron-Alcocer, A, Juarez-Ramirez, C, Ahuatzi-Chacon, D, Mondragon-Parada, ME & Galindez-Mayer, J (2009). Atrazine biodegradation by a bacterial community immobilized in two types of packed-bed biofilm reactors. World Journal Microbiology and Biotechnology, 25, 1995 - 2204.
3. Hayes, T., K. Haston, M. Tsui, A. Hoang, C. Haeffele, and A. Vonk. (2003). Atrazine induced hermaphroditism at 0.1 ppb in American leopard frogs (*Rana pipiens*): laboratory and field evidence. Environ. Health Perspect. 111, 568–575.
4. Hayes, T. B., A. Collins, M. Lee, M. Mendoza, N. Noriega, A. A. Stuart, and A. Vonk. (2002). Hermaphroditic, demasculinized frogs after exposure to the herbicide atrazine at low ecologically relevant doses. Proc. Natl. Acad. Sci. USA 99, 5476–5480.
5. Hayes, T. B., A. A. Stuart, M. Mendoza, A. Collins, N. Noriega, A. Vonk, G. Johnston, R. Liu, and D. Kpodzo. (2006). Characterization of atrazine-induced gonadal malformations in African clawed frogs (*Xenopus laevis*) and comparisons with effects of an androgen antagonist (cyproterone acetate) and exogenous estrogen (17 beta-estradiol): support for the demasculinization/ feminization hypothesis. Environ. Health Perspect. 114, 134–141.
6. Huff, J., and J. Sass. (2007). Atrazine—a likely human carcinogen? Int. J. Occup. Environ. Health 13, 356–358.
7. Bell, A. M., and N. C. Duke. (2005). Effects of Photosystem II inhibiting herbicides on mangroves—preliminary toxicology trials. Mar. Pollut. Bull. 51, 297–307.
8. Lockert, C. K., K. D. Hoagland, and B. D. Siegfried. (2006). Comparative sensitivity of freshwater algae to atrazine. Bull. Environ. Contam. Toxicol. 76, 73–79.
9. Belluck, D. A., S. L. Benjamin, and T. Dawson. (1991). Groundwater contamination by atrazine and its metabolites—risk assessment, policy, and legal implications. ACS Symp. Ser. 459, 254–273.

10. Gavrilescu, M. (2005). Fate of pesticides in the environment and its bioremediation. Eng. Life Sci. 5, 497–526.
11. Thurman, E. M., and M. T. Meyer. (1996). Herbicide metabolites in surface water and groundwater: introduction and overview. ACS Symp. Ser. 630, 1–15.
12. Van der Meer, J. R. (2006). Environmental pollution promotes selection of microbial degradation pathways. Front. Ecol. Environ. 4, 35–42.
13. Mandelbaum, RT, Wackett, LP & Allan, DL (1993) Rapid Hydrolysis of Atrazine to Hydroxyatrazine by Soil Bacteria. Environ Sci Technol*,* 27, 1943 - 1946.
14. Souza, MLd, Wackett, LP, Boundy-Mills, KL, Mandelbaum, RT & Sadowsky, MJ (1995) Cloning, characterization and expression of a gene region from *Pseudomonas* sp. strain ADP involved in the dechlorination of atrazine. Appl Environ Microbiol*,* 61, 3373-3378.
15. Martinez, B, Tomkins, J, Wackett, LP, Wing, R & Sadowsky, M (2001) Complete nucleotide sequence and organization of the atrazine catabolic plasmid pADP-1 from *Pseudomonas* sp. strain ADP J Bacteriol*,* 183, 5684 - 5697.
16. Strong, LC, McTavish, H, Sadowsky, MJ & Wackett, LP (2000) Field-scale remediation of atrazine-contaminated soil using recombinant *Escherichia coli* expressing atrazine chlorohydrolase. Environ Microbiol*,* 2, 91 – 98.
17. Seffernick, JL, McTavish, H, Osborne, JP, Souza, MLd, Sadowsky, MJ and Wackett, LP. (2002). Atrazine Chlorohydrolase from *Pseudomonas* Sp. Strain ADP Is a Metalloenzyme. Biochemistry**,** 41*,* 14430-14437.
18. Seffernick, JL, Souza, MLd, Sadowsky, MJ, Wackett, LP. (2001). Melamine deaminase and atrazine chlorohydrolase: 98 percent identical but functionally different. J. Bacteriol. 183, 2405–2410.
19. Shapir, N, Mongodin, EF, Sadowsky, MJ, Daugherty, SC,Nelson, KE, Wackett, LP. (2007). Evolution of catabolic pathways: genomic insights into microbial s-triazine metabolism. J. Bacteriol. 189, 674–682.
20. Wackett, LP. (1998). Directed evolution of new enzymes and pathways for environmental biocatalysis. Enzyme Eng. 864, 142–152
21. Seffernick, JL, Wackett, LP. (2001). Rapid evolution of bacterial catabolic enzymes: a case study with atrazine chlorohydrolase. Biochemistry 40, 12747–12753.

22. Scott, C, Jackson, CJ, Coppin, CW. (2009). Catalytic Improvement and Evolution of Atrazine Chlorohydrolase. Appl. Environ. Microbiol. 75(7), 2184-2191.
23. Wang, L, Samac, DA, Shapir, N, Wackett, LP, Vance, CP, Olszewski, NE, Sadowsky, MJ. (2005). Biodegradation of atrazine in transgenic plants expressing a modified bacterial atrazine chlorohydrolase (atzA) gene. Plant Biotechnol. J. 3, 475–486.
24. Kawahigashi, H, Hirose, S, Ohkawa, H, Ohkawa, Y. (2007). Herbicide resistance of transgenic rice plants expressing human CYP1A1. Biotechnol.Adv. 25, 75–84. 27.
25. Kawahigashi, H, Hirose, S, Ohkawa, H, Ohkawa, Y. (2006). Phytoremediation of the herbicides atrazine and metolachlor by transgenic rice plants expressing human CYP1A1, CYP2B6, and CYP2C19. J. Agric. Food Chem. 54, 2985–2991.
26. Alcalde, M, Ferrer, M, Plou, FJ, Ballesteros, A. (2006). Environmental biocatalysis: from remediation with enzymes to novel green processes. Trends Biotechnol. 24, 281–287.
27. Sutherland, TD, Horne, I, Weir, KM, Coppin, CW, Williams, MR, Selleck, M, Russell, RJ, Oakeshott, JG. (2004). Enzymatic bioremediation: from enzyme discovery to applications. Clin. Exp. Pharmacol. Physiol. 31, 817–821.
28. Souza, MLd, Sadowsky, MJ, Wackett, LP. (1996). Atrazine Chlorohydrolase from *Pseudomonas* sp. Strain ADP: Gene Sequence, Enzyme Purification, and Protein Characterization J. Bacteriol. 178, 4894-4900.
29. Seffernick, JL, Shapir, N, Schoeb, M, Johnson, G, Sadowsky, MJ, Wackett, LP. (2002). Enzymatic Degradation of Chlorodiamino-s-Triazine. Appl Environ Microbiol. 68(9), 4672–4675.
30. Berthelot, MPE. (1859). Rept. Chim. Appl. 1, 282.
31. Seffernick, JL, Johnson, G, Sadowsky, MJ, Wackett, LP. (2000). Substrate Specificity of Atrazine Chlorohydrolase and Atrazine-Catabolizing Bacteria. Applied And Environmental Microbiology 4247–4252.
32. Wackett, LP, Sadowsky, MJ, Martinez, B, Shapir, N. (2002). Biodegradation of atrazine and related s-triazine compounds: from enzymes to field studies. Appl Microbiol Biotechnol 58, 39–45.

33. Grcic, I, Koprivanac, N, Vujevi, D, Ujakov. Removal of atrazine herbicide from model wastewater. (2007). Wastewater Treatment in Small Communities and keynote speeches 335A.
34. Rietti-Shati, M, Ronen, D & Mandelbaum, RT (1996) Atrazine degradation by *Pseudomonas* strain ADP entrapped in sol-sel glass. J Sol-Gel Sci Technol 7, 77 - 79.
35. Kandimalla, VB, Tripathi, VS, Ju, H. (2006). Immobilization of Biomolecules in Sol–Gels: Biological and Analytical Applications. Critical Reviews in Analytical Chemistry 36, 73–10.
36. Reátegui, E & Aksan, A. (2009). Effects of the low temperature transitions of confined water on the structure of isolated and cytoplasmic proteins. J Phys Chem B 113, 13048-13060.
37. Nassif, N, Roux, C, Coradin, T, Bouvet, OMM & Livage, J. (2004). Bacteria quorum sensing in silica matrix. J Mater Chem, 14, 2264-2268.
38. Sambrook, J, Fritsch, EF, Maniatis, T. (1989). Molecular Cloning: A Laboratory Manual. Second edition. Cold Spring Harbor Laboratory Press. p.1.74.
39. Ca´novas, M, Torroglosa, T, Iborra, JL. (2005). Permeabilization of *Escherichia coli* cells in the biotransformation of trimethylammonium compounds into l-carnitine. Enzyme and Microbial Technology 37, 300–308.
40. Goswami, KP, Green, RE. (1971). Microbial Degradation of the Herbicide Atrazine and its 2-Hydroxy Analog in Submerged Soils. Environmental science and Tech. Vol. 5, Pages 426-4, 1.
41. Nassif, N, Bouvet, O, Rager, MN, Roux, C, Coradin, T, Livage, J. (2002). Living bacteria in silica gels. Nat Mater, 1, 42-44.
42. Perullini, M, Amoura, M, Roux, C, Coradin, T, Livage, J, Japas, ML, Jobbagy, M, Bilmes, SA. (2011). Improving silica matrices for encapsulation of *Escherichia coli* using osmoprotectors. J Mater Chem, 21, 4546 - 4552.
43. Pelekani, C, Snoeyink, VL. (2000). Competitive adsorption between atrazine and methylene blue on activated carbon: the importance of pore size distribution. Carbon, 38, 1423 - 1436.
44. Acosta, EJ, Steffensen, MB, Tichy, SE, Simanek, EE. (2004). Removal of water using covalent sequestration. J Agric Food Chem, 52, 545 - 549.

45. Bottero, JY, Khatib, K, Thomas, F, Jucker, K, Bersillon, JL, Mallevialle, J. (1994). Adsorption of atrazine onto zeolites and organoclays, in the presence of background organics. Water Res*,* 28, 483 - 490.
46. Yue, Z, Economy, J, Rajagopalan, K, Bordson, G, Piwoni, M, Ding, L, Snoeyink, VL, Marinas, BJ. (2006). Chemical activated carbon on a fiberglass substrate for removal of trace atrazine from water. J Mater Chem*,* 16, 3375 - 3380.
47. Devitt, E, Wiesner, MR. (1998). Dialysis investigations of atrazine-organic matter interactions and the role of a divalent metal. Environ Sci Technol*,* 32, 232 - 237.
48. Parra, S, Stanca, SE, Guasaquillo, I, Thampi, KR. (2004). Photocatalytic degradation of atrazine using suspended and supported TiO_2. Appl Catal, B*,* 51, 107 - 116.
49. Majewska-Nowak, K, Kabsch-Korutowicz, M, Dodz, M, Winnicki, T. (2002). The influence of organic carbon concentration on atrazine removal by UF membranes. Desalination*,* 147, 177 - 122.
50. Doulia, D, Hourdakis, A, Rigas, F, Anagnostopoulus, E. (1997). Removal of atrazine from water by use of nonionic polymeric resins. J Environ Sci Health, Part A*,* 32, 2635 - 2656.
51. Acero, JL, Stemmler, K, Gunten, Uv. (2000). Degradation kinetics of atrazine and its degradation products with ozone and OH radicals: a predictive tool for drinking water treatment Environ Sci Technol*,* 34, 591 - 597.
52. Livage, J, Coradin, T, Roux, C. (2001). Encapsulation of biomolecules in silica gels. J Phys: Condens Matter*,* 13, R673-R691.
53. Avnir, D, Coradin, T, Lev, O, Livage, J. (2006). Recent bio-applications of sol-gel materials. J Mater Chem*,* 16, 1013-1030.
54. Ferrer, ML, Yuste, L, Rojo, F, del Monte, F. (2003). Biocompatible sol-gel route for encapsulation of living bacteria in organically modified silica matrices. Chem Mater*,* 15, 3614-3618.
55. Depagne, C, Roux, C, Coradin, T. (2011). How to design cell-based biosensors using the sol–gel process. Anal Bioanal Chem 400(4), 965-976.
56. Kauffmann, C, Mandelbaum, RT. (1998). Entrapment of atrazine chlorohydrolase in sol-gel glass matrix. J Biotechnol*,* 62, 168 -176.

57. Hosticka, B, Norris, PM, Brenizer, JS, Daitch, CE. (1998). Gas flow through aerogels. J Non-Cryst Solids, 225, 293 - 297.
58. Blanch, HW, Clarke, DS, (1997). Kinetics of immobilized enzymes. Biochemical Engineering 103-161.
59. Pelekani, C, Snoeyink, VL. (2001). A kinetic and equilibrium study of competitive adsorption between atrazine and congo red dye. Carbon Volume 39, Issue 1, 25-37.
60. http://www.gsi-net.com/en/publications/gsi-chemical-database/single/37.html.
61. Kovaios, ID, Christakis, A, Paraskeva, Koutsoukos, PG, Payatakes, ACh. (2006). Adsorption of atrazine on soils: Model study; Journal of Colloid and Interface Science 299, 88–94.
62. Kovaios, ID, Christakis, A, Paraskeva, Koutsoukos, PG. (2011). Adsorption of atrazine from aqueous electrolyte solutions on humic acid and silica; Journal of Colloid and Interface Science 356, 277–285.